ANALYSIS OF INTERFERON-INDUCIBLE GENE EXPRESSION FOLLOWING RAS/RAF/MEK PATHWAY INHIBITION *in vivo*

AREZOO ALEMZADEH MEHRIZI

Analysis of Interferon-Inducible Gene Expression Following Ras/Raf/MEK pathway Inhibition *in vivo*

by

Arezoo Alemzadeh Mehrizi

A Thesis submitted to the

School of Graduate Studies

in partial fulfillment of the requirements for the degree of

Master of Science in Medicine

Division of Basic Medical Sciences, Faculty of Medicine

Memorial University of Newfoundland

July 2012

St. John's Newfoundland

ABSTRACT

Type I Interferons have been used to treat viral infections and cancer; however, IFN treatment is not always effective due to the presence of cellular suppressors of the IFN pathway such as Ras signalling activation. We have investigated whether inhibition of Ras signalling at the level of the MEK promotes the expression of IFN-inducible genes *in vivo*. BALB/c mice were injected intraperitoneally with either DMSO/PBS, an inhibitor for MEK (SL327, 100 mg/kg BW), IFN-α ($10x10^4$ U/mouse) or SL327/IFN-α combined. At 8 hrs after injection, the brain, intestine and lung were harvested for confirmation of MEK inhibition and semi-quantitative expression analysis for three IFN-inducible genes: *Gbp2*, *Rig-I* and *Stat2*. Western blot analysis of proteins isolated from SL327 treated lung showed reduced levels of phosphorylated substrate, indicating that the drug worked effectively to inhibit MEK *in vivo*. IFN significantly induced the expression of all genes in intestine and *Rig-I* in the brain; however, there was no significant induction of gene expression following the SL327 treatment and no synergistic effect was observed following the co-injection of SL327 and IFN-α. The results of this work suggest that MEK inhibition cannot effectively promote transcription of IFN-inducible genes under physiological conditions *in vivo*.

Acknowledgment

I would like to thank my supervisor Dr. Kenuske Hirasawa for giving me the opportunity to study cancer biology from the immunological perspective; for me, this was a new and interesting avenue of research.

I would like to take this opportunity to express my sincere appreciation to my supervisory committee members Dr. Ann Dorward and Dr. Mani Larijani for guiding me through all aspects of my program of study. Thank you for listening, encouraging and leading me in the right direction.

No matter where you are living, there are always people who make everywhere like home! I have made new friendships with wonderful people who possess dignity, generosity, and love in the heart. Thank you to my new friends: Firouzeh Nafar, Parisa Modirrousta, Ghazal Assadipour, Mahdis Monajemi and Peyvand Amini.

I wholeheartedly send out my tremendous thanks and appreciation to my beloved parents for their sincere and endless love, encouragement and support. I am so grateful for their efforts to provide me with the best environment for growing up, and inspiring me with the confidence that all dreams are possible. Finally, I wish to dedicate this work to my beloved Grandma, whom I love and miss.

Table of Contents

List of Tables

List of Figures

List of Abbreviations

2'5'-OAS	2'5'-Oligoadenylate synthetase
APS	Ammonium persulfate
BCA	Bicinchoninic acid
bp	Base pair
BW	Body weight
°C	Centigrade
c-Myc	Myelocytomatosis viral oncogene homolog
CARD	Caspase recruitment domain
Chr	Chromosome
CNS	Central nervous system
CML	Chronic myeloid leukemia
CTD	C-terminal domain
DMSO	Dimethyl sulfoxide
DC	Dendritic cells
dsRNA	Double-stranded RNA
EMCV	Encephalomyocarditis virus
ERK	Extra cellular signal-regulated kinase
GAP	GTPase activating proteins
Gapdh	Mouse Glyceraldehyde 3-phosphate dehydrogenase (Gapdh: Protein; *Gapdh*: Gene)

GAPDH	Human Glyceraldehyde 3-phosphate dehydrogenase (GAPDH: Protein; *GAPDH*: Gene)
Gbp2	Mouse Guanylate binding protein 2 (Gbp2: Protein; *Gbp2*: Gene)
GBP2	Human Guanylate binding protein 2 (GBP2: Protein; *GBP2*: Gene)
GDP	Guanylate diphosphate
GEF	Guanine nucleotide exchange factor
g	Gram
GTP	Guanylate triphosphate
h	Hour
HBV	Hepatitis B virus
HCL	Hairy cell leukemia
HCV	Hepatitis C virus
HIV	Human immunodeficiency virus
hrs	Hours
HSV	Herpes simplex virus
IgG	Immunoglobulin G
IFNs	Interferons
IFNR	IFN-α receptor
IL-1R	Toll-interleukin 1 receptor
IP	Intraperitoneally
IPS-1	IFN-β promoter stimulator-1
IRF	Interferon regulatory factor

ISGs	Interferon stimulated genes
ISGF3	IFN-stimulated gene factor 3
ISRE	IFN-stimulated response element
Jak	Janus family of tyrosine kinases
Jak-STAT	Janus activated kinase-signal transducer and activation of transcription
kDa	Kilodalton
Kg	Kilogram
l	Liter
LRR	Leucine-rich-repeat
M	Molar
MDII genes	MEK-mitogen-activated protein/extra cellular signal-regulated kinase
MHC	Major histocompatibility complex
min	Minutes
mg	Milligram
ml	Millilitre
mM	Millimolar
MMP9	Matrix metalloprotein 9
My88	Myeloid differentiation primary response gene 88
Mx	Myxovirus resistance gene
NA	Not assessed
ng	Nanogram

NK	Natural killer cells
nm	Nanometre
NTP	Nucleotide Triphosphate
p-ERK	Phospho-ERK
P53	protein 53
PBS	Phosphate buffered saline
PIAS	Protein inhibitor of activated STAT
PKR	dsRNA-activated protein kinase
PPP	Triphosphate
q-PCR	Quantitative PCR
Ras	Rat Sarcoma virus oncogene
RCL	Renal cell carcinoma
RD	Repressor domain
Rig-I	Mouse Retinoic acid inducible gene-I (Rig-I: Protein; *Rig-I*: gene)
RIG-I	Human Retinoic acid inducible gene-I (RIG-I: Protein; *RIG-I*: gene)
RNAase L	Latent ribonuclease
RNAi	RNA interference
RSV	Respiratory syncytial virus
RT-PCR	Real time-polymerase chain reaction
RTK	Receptor tyrosine kinases
SDS-PAGE	Sodium dodecyl sulfate-polyacrylamide gel Electrophoresis

SEM	Standard error of the mean
SH2	Src-homology 2
SHP	SH2 containing phosphatases
SOCS	Suppressors of cytokine signalling
Stat2	Mouse Signal transducer and activation of transcription (Stat2: Protein; *Stat2*: Gene)
STAT2	Human Signal transducer and activation of transcription (STAT2: Protein; *STAT2*: Gene)
ssRNA	Singled-stranded RNA
t-ERK	Total-ERK
TBK	TANK-binding kinase 1
TBST	Tris-buffered saline with tween
TEMED	Tetramethylethylenediamine
Th-1	T helper-1
TIR	Toll-interleukin 1 receptor homology
TLR	Toll-like receptor
TNF	Tumor necrosis factor
TRIF	TIR-domain-containing adaptor-inducing IFN
Tris-HCl	Tris (hydroxymethyl) aminomethane-hydrochloride
V	Volts
VSV	Vesicular stomatitis virus
xg	Times gravity
µg	Microgram

µl	Microliter

Chapter 1: Introduction

1.1 INTERFERONS

Interferons (IFNs) are cytokines best recognized for their pivotal role in antiviral defence in mammals (1, 2). IFNs were discovered by Isaacs and Lindenmann (1957) while they were studying the mechanisms of antiviral defence, and recognition of their ability in interfering with viral infection led to their nomination as "interferons" by these scientists (3). In contrast to antiviral drugs used at that time, IFNs had almost no toxicity and acted against a wide range of viruses. These unique properties made them superior over common antiviral substances, which encouraged virologists to further investigate and expand their knowledge of IFN biology (1, 2, 4). IFNs were the first cytokines identified, purified, cloned, sequenced, and produced in recombinant form for clinical use (3, 5-7).

IFNs are a group of pleiotropic cytokines with antiviral, antitumor, and immunomodulatory functions (1-3). Based on the range and importance of their activities, IFNs have been used for the treatment of various pathological conditions, including certain viral infections, several types of cancer and autoimmune diseases (8-12). The biological functions and subsequent interventional properties of IFNs are mediated by the IFN stimulated genes (ISGs), which comprise a large group of genes with great diversity in function (Table 1.1) (13). They are classified into three groups according to their receptor specificity and amino acid sequence homology as type I, type II and type III IFNs (14).

Table 1.1 Gene ontology classifications of ISGs

Functional Categories
Adhesion
Angiogenesis
Antigen presentation
Antigen processing
Antiviral
Apoptosis
Cancer
Cell-cell adhesion
Cell cycle
Chemokine
Cytoskeleton
Development
DNA replication/repair
Extracellular matrix
G-protein signalling
Growth factor
GTP-binding
Host defense
Immune modulation
Inflammation
Lymphocyte adhesion
Oncogene
Protease
Protease inhibitor
RNA splicing
Transcription factor
Transcriptional activator
Transcriptional repressor
Translation
Tumor suppressor
Ubiquitination
Vesicle transport

Adapted from reference (13)

1.1.2 Type I Interferons

Type I IFNs are a multi-gene family comprised of eight subclasses in mammals: IFN-α, IFN-β, IFN-ε, IFN-κ, IFN-ω, IFN-τ, IFN-δ, and IFN-ζ (Table 1.2) (15, 16). Each gene is encoded by a single exon on human chromosome (Chr) 9, and mouse Chr 4 (17). The size of type I IFNs ranges from 165-200 amino acids and their sequence homology ranges from 30-80 % within species (6, 15, 16). IFNs activate intracellular signalling networks in an autocrine and paracrine manner by binding to hetero-dimeric cell surface receptors, IFN-α receptor (IFNR)1 and IFNR2 , which are distributed in all human cell types (1, 18, 19). Antiviral, immunomodulatory, and antitumor actions are the main functions of the type I IFNs (1, 2).

In mammals, type I IFNs are considered the principal antiviral cytokines with significant regulatory roles in innate and adaptive immune responses. To induce innate immune responses, they act directly on uninfected or virally infected cells, which leads to inhibition of viral nucleic acid replication and mRNA translation (20). Type I IFNs accomplish this by signalling the up-regulation of ISGs that mediate the antiviral attack. Examples of antiviral ISGs are: 2'5'-Oligoadenylate synthetase (OAS), dsRNA-activated protein kinase (PKR) and Myxovirus resistance gene (Mx), which play important roles in type I IFN-induced innate immunity (2). The antiviral activity of 2'5'-OAS targets viral RNA, while PKR targets viral translation, and Mx targets viral replication.

Table 1.2 Expression pattern of type I IFNs in mammals

Expression pattern	**Type I IFN subtypes**
Ubiquitously expressed	α1, α2, α3, α4, α5, α6, α7, α8, α10, α13, α14, α16, α17, α21, β
Leukocytes	ω [a]
Uterus, Ovary	ε
Epidermal keratinocytes	K
Trophoblast	τ[b], δ[c]
Spleen, thymus, lymph node	Z

[a] Absent in mice; [b] Ruminants only; [c] Pigs and cattle only

Adapted from references (15) and (16)

2'5'-OAS activates a latent ribonuclease termed RNAase L, leading to degradation of host and viral RNA (21). PKR inhibits viral translation through phosphorylation and subsequent inactivation of eukaryotic initiation factor 2α (22). Mx blocks viral replication via inhibition of viral translocation across the nuclear membrane (23).

Type I IFN-induced adaptive immunity is mediated through their immunomodulatory functions and subsequent promotion of antigen presentation and pathogen clearance stages (24, 25). Type I IFNs enhance the process of antigen presentation through induction of differentiation of T-helper (Th)-1 cells (26), differentiation and activation of dendritic cells (DC) and increased expression of major histocompatibility complex (MHC) Class I and MHC II (27, 28). Their promotional role to stimulate the formation and activity of cytotoxic T lymphocytes (29, 30), induction of macrophage (31) and natural killer cells (NK) activity (32, 33) facilitates elimination of virally infected cells. Notably, these immunomodulatory functions highlight the importance of type I IFNs to bridge the innate and adaptive immune responses, which emphasizes their quality as strong antiviral effectors.

Type I IFNs induce antitumor responses through direct and indirect effects on tumor cell growth and progression. Directly, they reduce oncogene expression such as Myelocytomatosis viral oncogene homolog (c-Myc), and they induce tumor suppressor gene expression such as the tumor necrosis factor (TNF) receptor family and protein 53 (P53) (4, 21). Indirectly, the antitumor effects of type I IFNs are mediated by increased immune-mediated tumor surveillance and down-regulation of proangiogenic molecules (34, 35). The immunomodulatory functions of type I IFNs also cause stimulation of

adaptive immunity responses against tumor cells, which promote host immune recognition and eradication of emerging tumor cells. In addition, both IFN-α and IFN-β down-regulate several important proangiogenic molecules such as matrix metalloprotein (MMP9), vascular endothelial growth factor, and basic fibroblast growth factor to restrict blood vessel supply (36). Through their broad immunoregulatory and antiangiogenic activities, type I IFNs suppress tumor initiation and progression. This is the basis for clinical research initiatives that incorporate type I IFNs into antitumor therapeutic strategies (34).

1.2 TYPE I IFN PRODUCTION PATHWAYS

In mammalian organisms, the first step to control viral infection is detection of these pathogens, which subsequently triggers induction of innate immune responses. The sensing of viruses and subsequent induction of type I IFNs is mediated by two pathways: the Retinoic acid inducible gene-I (RIG-I)-dependent pathway and the Toll-like receptor (TLR)-dependent pathway (37, 38). These pathways show some cell specificity; for example, type I IFN production in macrophages and DC is mediated through TLR-dependent pathways (39-41) and in other types of cells, including both immune and non-immune, is stimulated by RIG-I-dependent pathway (39, 41-43). Several transcription factors can be activated by RIG-I and TLR pathways through different mechanisms, but the production of type I IFNs is stimulated by activation of Interferon regulatory factor (IRF)3 and IRF7 (44, 45).

1.2.1 RIG-I dependent pathway for IFN induction

RIG-I (DDX58) functions as a cytoplasmic sensor for different types of RNA viruses, including singled-stranded RNA (ssRNA) viruses harbouring a 5'-Triphosphate (5'-PPP) group (46-48) and double-stranded RNA (dsRNA) viruses (49, 50). RIG-I belongs to DEAD (Asparagine-Glutamine-Alanine-Histamine/Asparagine)-box RNA helicase family (43). This family of proteins use nucleotide triphosphate (NTP)s as source of energy to mediate a variety of functions such as translation, transcription, mRNA splicing and RNA decay (51, 52). RIG-I consists of four functional domains: two amino-terminal caspase recruitment domains (CARD) (43, 53), a central DEAD-box helicase domain (43, 54, 55) and a C-terminal domain (CTD) also known as the repressor domain (RD) (50, 53, 56, 57). The CARD domains are responsible for transmitting the signal from RIG-I to downstream signalling molecules; the DEAD-box helicase domain is responsible for both RNA recognition and providing energy for conformational changes through the hydrolysis of ATP; the CTD/RD domain is responsible for both inhibition of RIG-I signalling and recognition of RNA viruses. RIG-I is inactivated in the absence of viral RNA, and in this state the CARD domain is masked by CTD/RD domain to repress signalling to downstream molecules (Figure 1.1) (58). Viral binding to CTD/RD or DEAD-box domains activates ATPase activity leading to the unmasking of CARD domains and activation of signalling (50, 59). The CARD domain of activated RIG-I interacts with the CARD domain of a mitochondrial antiviral signalling protein (MAVS) also termed IFN-β promoter stimulator 1 (IPS-1) or VISA or CARDIF (25, 60).

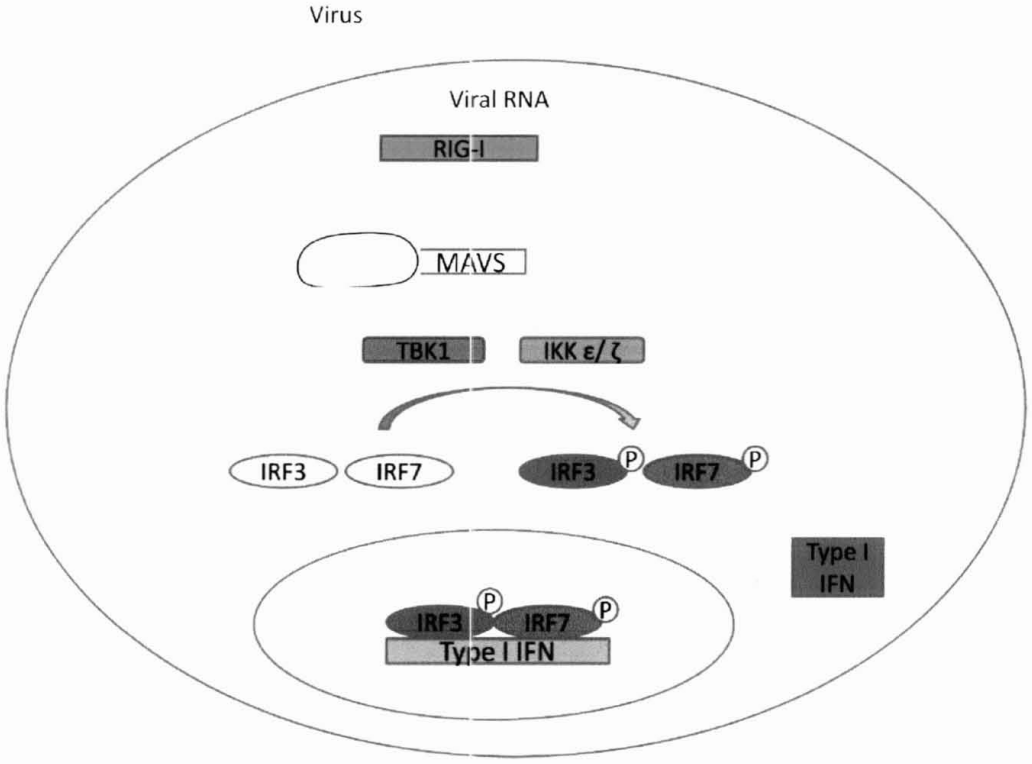

Figure 1.1 RIG-I dependent production of type I IFNs. Binding of virus to RIG-I induces conformational changes and its subsequent activation. Activated RIG-I induces activation of MAVS which in turn activates TBK1 and IKKε through phosphorylation. After phosphorylation by TBK1 and IKKε, IRF3 and IRF7 translocate to the nucleus and induce transcription of Type I IFNs.

Activated IPS-1 relays the signal to the TANK-binding kinase 1 (TBK1) and inducible IκB kinase (IKK-i; also known as IKKε), which phosphorylate IRF3 and IFR7 (61, 62). Phosphorylated IRF3 and IRF7 translocate to the nucleus to activate transcription of type I IFNs (44, 45).

1.2.2 TLR-dependent pathway for IFN induction

TLRs are a family of trans-membrane proteins that sense different types of pathogens at the cell surface or in the endosome (63-66). Among TLRs, TLR3, TLR7, TLR8 and TLR9 are localized in the endosome and are able to induce Type I IFN dependent antiviral responses (37, 67). The best known ligand for TLR3 is dsRNA, for TLR7/8 is ssRNA and for TLR9 is viral DNA or bacterial DNA with a CpG motif (68-75). In all TLRs, recognition of viral particles is mediated by the leucine-rich-repeat (LRR) domain, and they also posses the Toll-interleukin 1 receptor (IL-1R) homology (TIR) domain, which is a docking site for downstream adaptor proteins (Figure 1.2) (76-79). The TIR-domain-containing adaptor-inducing IFN (TRIF) serves as an adaptor protein for TLR3 signalling, while Myeloid differentiation primary response Gene 88 (My88) serves as an adaptor protein for TLR7, TLR8 and TLR9 signalling (80, 81). These adaptor proteins activate TBK1 and IKKε (82, 83), which in turn phosphorylate IRF3 and IRF7 (61, 62). Phosphorylated IRF3 and IRF7 subsequently translocate to the nucleus to activate transcription of type I IFNs (44, 45).

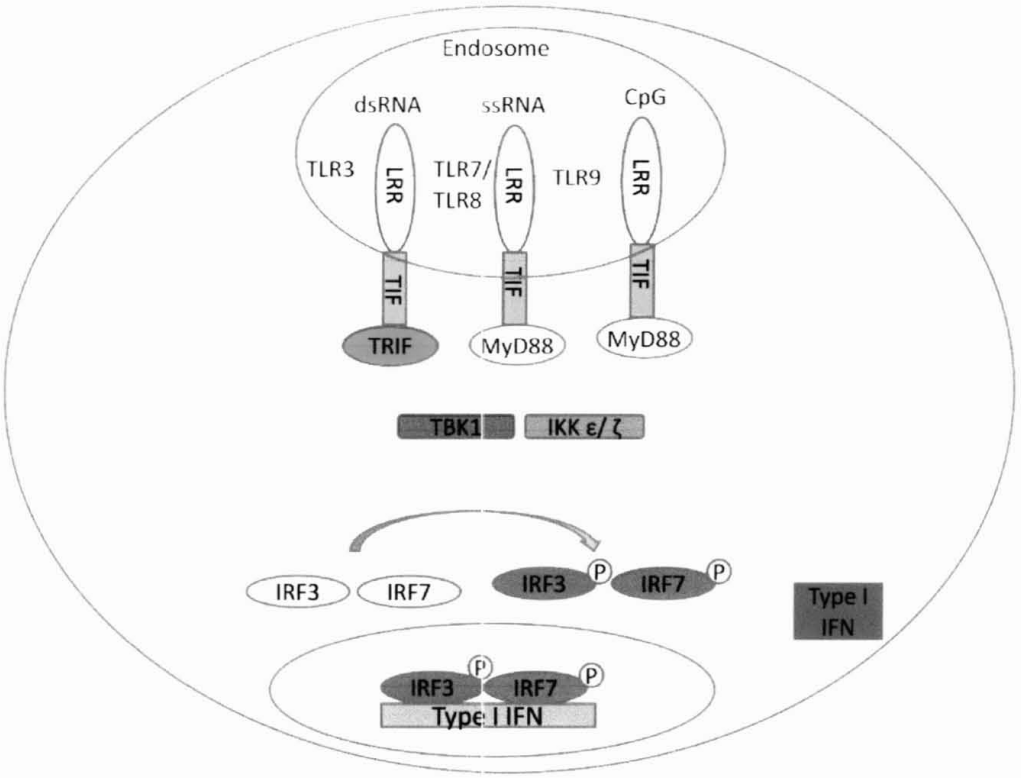

Figure 1.2 The TLR-dependent production of type I IFNs. Binding of viral products (ssRNA, dsRNA, CpG) to the LRR domain of the TLRs resulted in their activation. Upon activation, TLR3 activated its downstream adaptor protein TRIF while MyD88 is the downstream target of TLR7, TLR8, and TLR9. Upon activation, TRIF and MyD88 activate TBK1, and IKKε which phosphorylate IRF3 and IRF7. Following phosphorylation, they translocate to the nucleus and induce transcription of Type I IFNs.

1.3 TYPE I IFN SIGNALLING PATHWAY

IFNs serve to establish an antiviral state in the host organism following viral infection. Following their secretion from virally infected cells, IFNs act in both an autocrine and paracrine manner to up-regulate ISGs in both infected and non-infected neighboring cells (84). A well recognized signaling pathway important for relay of type I IFN actions is the Janus activated kinase-signal transducer and activation of transcription (Jak-STAT) pathway (2, 85-87). Members of the janus family of tyrosine kinases (Jak) and signal transducer and activator of transcription (STAT) proteins are the principal components of Jak-STAT pathway that can be induced by several cytokines besides IFNs. Jak1 (88) and Tyk-2 (89-91) of the Jak family, and STAT1 (92, 93) and STAT2 (94-96) of the STAT family, play central roles in type I IFN signaling (20).

Autocrine or paracrine IFN signaling is triggered by binding of type I IFNs to their hetero-dimeric cell surface receptors comprised of one IFNR1 and one IFNR2 subunit. Intracellularly, IFNR1 is associated with Tyk-2 and IFNR2 is associated with Jak1 (97-99), such that IFN binding stimulates transphosphorylation and subsequent activation of Tyk-2 and Jak1, respectively (Figure 1.3) (98, 100). Activated Jak1 and Tyk2 phosphorylate their associated receptors on their tyrosine residues in the cytoplasmic domain. Phosphotyrosyl residues act as a docking site to recruit STAT2 (96, 101) leading to STAT2 phosphorylation by Jak1 and Tyk-2, which accelerate phosphorylation of STAT1 by these kinases (2, 102). Once phosphorylated, STAT1 and STAT2 form heterodimers, which in turn bind to IRF9 and form a trimeric complex termed IFN-stimulated gene factor 3 (ISGF3) (20, 103).

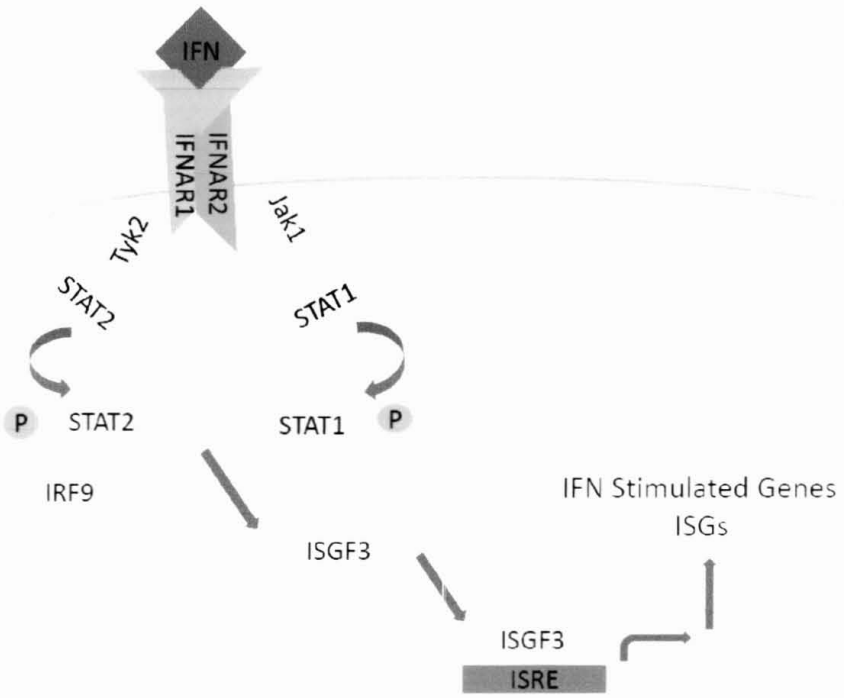

Figure 1.3 Type I IFN signalling pathway. Type I IFNs bind and activate IFNR1 and IFNR2 which in turn activate Tyk2 and Jak1, leading to phosphorylation of STAT2 and STAT1. Phosphorylated STAT2 and STAT1 form heterodimers which binds to IRF9 and forms a trimeric complex named ISGF3. ISGF3 translocates to the nucleus and activates transcription of IFN-inducible genes.

ISGF3 translocates to the nucleus and binds to the IFN-stimulated response element (ISRE) in the promoter of ISGs to induce their expression (2, 104).

1.4. MULTIFUCTIONAL ISGS WITH PIVOTAL ROLES IN TYPE I IFN SIGNALLING

1.4.1 GBP2

GBP2 is one member of the GBP family, which are one class of the type I IFN-induced guanosine triphosphatase. Their naming as GBP is based on their capacity to bind agarose-immobilized guanine nucleotides (105-107). GBP2 is a cytoplasmic protein that was first identified from a cDNA library obtained from type I and type II IFN-treated human fibroblast cells in 1991 (108). GBP2's high rate of induction (> 6 fold) following exogenous type I and type II IFN has led to its recognition as one of the markers of IFN responsiveness (105, 106, 109-112). There is evidence for both antiviral and antitumor properties for GBP2. The antiviral activities of GBP2 were first identified by Carter *et al.* in 2005. They showed GBP2 has antiviral activity against vesicular stomatitis virus (VSV) and encephalomyocarditis virus (EMCV) (109). GBP2 mediated its antiviral activities against VSV in a GTPase-dependent manner and against EMCV in a GTPase independent manner (109). In addition, GBP2 was one of the up-regulated genes in lungs of pigs infected with Porcine Circovirus type 2 (113). Fernandes *et al.* suggested the antiviral activity of GBP2 against this virus is mediated through T-cell activation, which implies an immunomodulatory role and GBP2 involvement in adaptive immunity (113). The antitumor functions of GBP2, which were discovered in the context of type II IFN

signalling, are also mediated through down regulation of an angiogenic factor, MMP9, and down regulation of a cell migration factor, Rac (114, 115). Overall, evidence suggests a broad range of activities for GBP2, pivotal for antiviral and antitumor responses induced by IFNs.

1.4.2 RIG-I

In 1997, RIG-I was identified as one of the genes that mediates all-trans retinoic acid-induced differentiation of acute promyelocytic leukemia cells (116). In 2004, Yoneyama *et al.* recognized antiviral properties of RIG-I (117). They found that it triggered production of type I IFNs through sensing of RNA viruses. Interestingly, its expression is also under regulation by IFNs; therefore, RIG-I is categorized as an ISG which enables RIG-I to further promote innate immune responses in a positive feedback loop (117). RIG-I is a key component of IFN production, as many positive and negative regulators of the IFN pathway exert their effects at the level of this protein (39, 118, 119). RIG-I is ubiquitously expressed in most cell types and recognizes RNA viruses with specific molecular features, including: 5'-PPP, ssRNA, dsRNA forms. This is hypothesized to be a practical strategy for cells to discriminate self RNA molecules from non-self RNA and thus prevent autoimmune reactions (42, 54, 58, 118). More than twenty RNA viruses are known to be recognized by RIG-I, including some that have severe effects on human health, including: hepatitis C virus (HCV), human immunodeficiency virus (HIV) and influenza virus (Table1.3) (39, 117, 120).

Table 1.3 RNA viruses sensed by RIG-I

Family	Viruses
Rhabdoviridae	Reoviridae, Rabies virus
Paramyxoviridae	Sendai virus, New Castle disease virus, Respiratory syncytical virus, Measles virus, Nipah virus
Orthomyxoviridae	Influenza A virus, Influenza B virus
Filoviridae	Ebola virus, Hepatitis C virus, Japanese encephalitis virus, Dengue virus, West Nile virus
Arenaviridae	Lassa virus
Bunyaviridae	Rift Valley fever virus
Reoviridae	Orthoreovirus

Adapted from references (39), (117), (120)

Since the activation of innate immunity is a critical step for mounting long term adaptive immunity, RIG-I can be considered an indirect stimulator of adaptive immunity. In addition to this indirect influence, the immunomodulatory functions of RIG-I on DC (121), T-cells (56), NK cells (122) and MHC1 expression (123), directly induce adaptive immunity against virally infected cells and tumor cells. The antitumor potential of RIG-I was first identified by Zhong Su *et al.* in 2007 (124). They observed lower expression of this protein in several cancer models, including prostate, breast, melanoma and malignant glioma cancer cell lines when compared to normal cell lines of equivalent tissue. The antitumor functions of RIG-I are mediated through apoptotic (122, 125-127) and anti-proliferative (128) activities, thus reduced expression of RIG-I would permit apoptosis evasion and excessive proliferation, common characteristics of tumor cells.
Overall, RIG-I has a significant impact on cellular signalling integration with a major impact on host health, which has encouraged both virologists and cancer researchers to focus on this protein for the development of interventional therapeutic approaches (39, 118, 119, 127).

1.4.3 STAT2

STAT2 was first identified by Fu *et al.*, while they were exploring the polypeptide composition of the ISGF3 complex in 1990 that was already recognized as a key component of the IFN response (129). Several loss of function studies demonstrated the potential of STAT2 as an essential component of type I IFN signalling. Leung *et al.* found that cells lacking STAT2 have defective type I IFN response (95). In two other

independent studies, it was found that *Stat2* knockout mice are more vulnerable to many types of viruses (130, 131). There are two themes of type I IFN signalling pathway, in both of which STAT2 is a key transcription factor: 1) the classic pathway, described at section 1.3, includes STAT2, STAT1 and IRF9; 2) the non-classic pathway includes STAT2 and other transcription factors rather than STAT1 and IRF9. In terms of the classic signaling pathway, there are two features already defined: 1) required level of STAT2 phosphorylation or threshold that is required for phosphorylation of STAT1 and subsequent formation of active ISGF3 (102); 2) requirement of STAT2 for interacting with additional transcription factors and regulators of type I IFN signalling (132-134). There are some type I IFN-induced non-classic Jak-STAT signalling pathways, for which STAT2 is a pivotal transcription factor: 1) STAT2 mediates signalling in a STAT1-independent manner through an active STAT2:IRF9 complex (135-137); 2) STAT2 mediates signalling in an IRF9-independent manner through a STAT2:STAT1 complex (138); 3) STAT2 mediates signalling in a STAT1/IRF9 independent manner (STAT2:STAT3 complex, STAT2:STAT6 complex) (110, 139). All above examples suggest the dependency of type I IFN signalling function to STAT2 rather than to STAT1 and IRF9.

Like RIG-I, Yan *et al.* (1995) found that STAT2 is also an ISG, and thereby amplifies type I IFN responses (91). STAT2 is essential for adaptive immunity against viral and tumor cells of macrophage (31), DC (140), and Th cells (141). The first observation of antitumor activity of STAT2 comes from a study in 2003, which showed *Stat2* knockout mice developed brain tumors (142). In addition, loss of STAT2

accompanied tumor progression characteristic in colorectal, renal, and melanoma cancer cells (143, 144). STAT2 also plays critical roles for inducing apoptosis of tumor cells (144-146), inhibition of cell growth (140, 147) and down-regulation of an angiogenic factor MMP9 (148). Overall, by its determinant role in type I IFN signalling and modulating vital biological process, STAT2 can be considered one of the most prominent ISGs, important for fidelity of type I IFN signalling and health.

1.5. IFN THERAPY AND ITS LIMITATIONS

1.5.1 IFN therapy

Based on their pivotal physiological roles, IFNs, especially type I IFNs, have achieved a notable role in clinical medicine following their recombinant production in 1980 (1, 2). Their first entry in clinics occurred in 1985 for treatment of hairy cell leukemia (HCL), 28 years after their discovery (149). Since then, they have been approved as a treatment for viral infections, cancer, and multiple sclerosis (MS) as an autoimmune disease (20, 149).

Of viral diseases, type I IFNs were approved for treatment of HBV (150), HCV(151), herpes simplex virus (HSV) (152), HIV (153, 154), herpes zoster (155), and common cold viruses (156, 157), but now they are applied just for treatment of HBV and HCV. HBV is a serious international public health problem, with approximately 400 million people infected throughout the world (158). This infection causes severe symptoms including liver cirrhosis and hepatocellular carcinoma, thereby leading to

chronic and deadly disease outcomes (159-161). IFN-α was introduced as the first intervention for HBV in 1991 (162). In the past two decades, IFN-α has been recognized as an effective treatment, as it causes a reduction in disease severity in about 25-40% of patients (163, 164). HCV currently infects 175 million people world-wide and induces the same symptoms and outcomes as HBV (165). The treatment of chronic HCV with IFNs began with sole application of IFN-α, to which 20% of patients responded (166). Co-administration of IFN-α2 with low dose of the antiviral drug ribavirin led to a synergistic effect and increased response rates to 40% of patients (167). Current form of treatments includes application of long-acting, pegylated IFN-α2 with ribavirin which has led to improvements-over 60% of patients are cured (168). Pegylated IFN-α2 consists of polyethylene glycol added to the IFN-α2, a chemical modification which increases IFN-α2 half life and duration of activity (169).

Type I IFNs are an important treatment option for MS, which is an autoimmune disease. In this disease, neural transmission in the central nervous system (CNS) becomes aberrant as a result of demyelination of CNS. This is a consequence of autoimmune reactions against myelin (170-172). MS patients suffer from muscle weakness, muscle spasms or difficulty in moving, difficulties with coordination and balance and visual problems (173, 174). IFN-β is the main immunomodulatory medication for this disease, and its clinical benefits are observed in 50-75% patients (175). It reduces CNS inflammation, and thereby reduces symptoms of physical disability (176). The molecular mechanisms through which IFN-β exerts its clinical benefits are not well understood. It is

hypothesised that those effects are mediated through immunomodulatory function of IFN-β (176).

Even though type I IFNs are best recognized for their unique antiviral properties, they first entered into the clinic as an antitumor therapeutic agent for HCL in 1985 (177). Further investigations revealed their antitumor activity against some other types of cancer, which ultimately led to their application for treatment of chronic myeloid leukemia (CML), B- and T-cell Lymphomas, melanoma, renal cell carcinoma (RCL) and Kaposi's sarcoma (149). Although for some cancers such as CML and HCL, type I IFNs are delegating their place to some new anticancer drugs, they are still widely used for treatment of some malignancies such as melanoma (34). Since 1995, IFN-α has been used as an adjuvant therapy for patients with high risk melanoma (178, 179). It benefits these patients with increased disease-free survival for about 9 months, and overall survival by 8-9% (180, 181).

1.5.2 Limitations of IFN therapy

Type I IFNs have shown promise for the treatment for some life threatening and debilitating diseases; however, their overall therapeutic efficacy is only moderate (1, 2). One obstacle to the success of IFN therapy is the phenomenon of patient resistance to IFN treatment. Given the potential of IFN therapy, understanding the obstacles to success of IFN therapy might improve therapeutic outcomes. Three factors are associated with IFN resistance: 1) genetic alterations of components involved in IFN production or IFN signalling pathways (182-184); 2) anti-IFN proteins encoded by viral genomes (185,

186); and 3) elevated activities of endogenous cellular suppressors of IFN signalling (187-190).

Mutations or polymorphisms of IFN signaling components can change IFN susceptibility from responsive to non-responsive phenotype. For example, defective STAT1 expression correlates with IFN-α resistance in CML and a cutaneous T-cell lymphoma cell line (183, 184). In addition, Shang *et al.* found that abolished Jak1, Tyk2 and Stat1 expression leads to impairment of Jak-STAT signalling, which underlies IFN resistance in RCL cell lines (182). Recognition of impacts of mutations of different type I IFN signalling will open an avenue for developing markers for future personalized therapy decisions.

Viruses have developed strategies to shut down IFN signalling in order to evade innate immune responses and support viral propagation. Viruses may counteract IFN-mediated antiviral defences in either a direct or indirect manner (185, 187). Directly, viruses encode proteins which disrupt the IFN signalling pathway through targeting its components. For instance, Dengue virus encodes a protein which binds to STAT2 leading to its ubiquitination and subsequent degradation (191). Another example is suppression of RIG-I signalling by HCV; this virus encodes a protease which cleaves IPS-1 from mitochondria (192). Indirectly, viruses exploit cellular suppressors of IFN signalling to attenuate IFN response (193, 194). Viruses lacking anti-IFN proteins propagate selectively in cells with elevated activity of these cellular inhibitors, thereby causing more severe diseases in humans and animals (195-197). The up-regulation of endogenous suppressors of IFN signalling was also observed in cancer cells resistant to IFN (189,

190). This evidence suggested these are serious barriers to IFN therapy efficacy and the suppressor mechanisms have been the focus of recent research.

1.6. CELLULAR SUPPRESSORS OF IFN SIGNALLING

The primary function of endogenous cellular suppressors of IFN signalling is to maintain the homeostasis of IFN signal transduction (187), as prolonged or constitutive activation of IFNs leads to destructive biological consequences such as asthma, fatigue, and depression (198, 199). Three major families of type I IFN signalling pathway inhibitors include: Src-homology 2 (SH2)-containing phosphatases (SHP), the suppressors of cytokine signalling (SOCS) family and protein inhibitor of activated STAT (PIAS) (Figure 1.4) (187). Activation of Ras/Raf/MEK pathway also was recognized as inhibitor of IFN signalling in our laboratory (197).

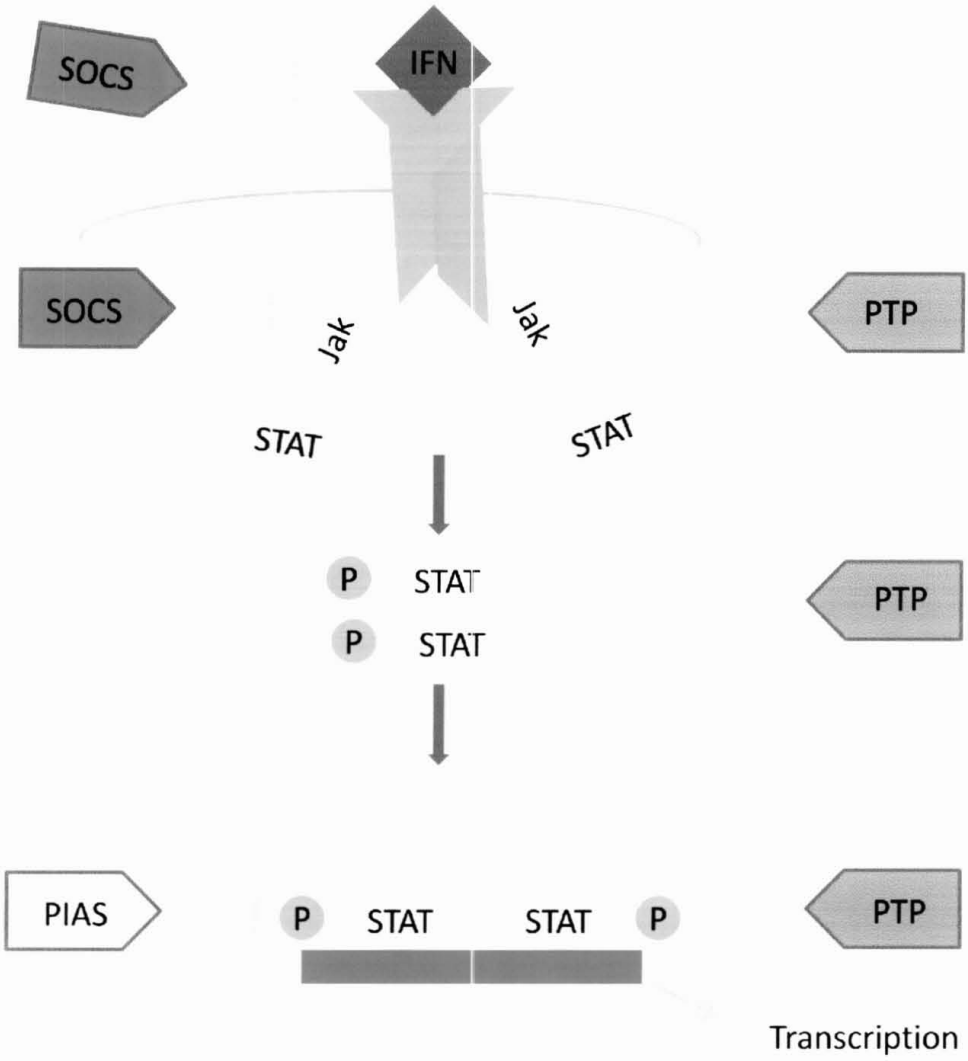

Figure 1.4 Suppressors of IFN signalling. The SOCS family members suppress Jak kinases activity, or act as a competitor of IFN in binding to receptors. PTP family members de-phosphorylate Jaks and STAT1 to induce ubiquitin-mediated degradation of Jaks. PIAS family members prevent transcriptional activity of STAT dimers.

Phosphorylation is an integral feature of the activated Jak-STAT signalling cascade, such that de-phosphorylating events offer the cell a significant level of control. SHP1 and SHP2 are tyrosine phosphatases involved in the negative regulation of type I IFN signalling (200). SHP1 attenuates type I IFN signaling through de-phosphorylation of JaK1 (201, 202), while SHP2 induces the same suppression through de-phosphorylation of STAT1 (202, 203). Sodium stibogluconate is an inhibitor of both SHP1 and SHP2 and its combination with IFN-α showed significant synergistic effect on IFN-α responsiveness in both *in vitro* and *in vivo* experiments (204, 205). This combination entered into phase I trials for evaluating safety and target inhibition for treatment of melanoma (206).

The SOCS family is comprised of eight members, including: cytokine inducible SH2 containing protein and SOCS 1-7 (207). Generally, their inhibitory effects are mediated via three mechanisms: as antagonists for STAT binding to phosphorylation target sites on receptors, inducers of proteosomal degradation of bound signalling proteins and suppressors of Jak activity through a binding interaction (208). Among the SOCS family, SOCS1 and SOCS3 are involved in the negative regulation of type I IFN signalling (209). Up-regulation of SOCS3 is one of the strategies used by Influenza A virus and HIV to suppress type I IFN signalling (210, 211). The same mechanism is used by HSV, as it induces SOCS1 or SOCS3 for evading IFN-induced immunity (193, 212). In addition, over expression of SOCS3 was observed in myelogenous leukemia cells resistant to IFN-α (189). The levels of both SOCS1 and SOCS3 activity are determinant factors of IFN-susceptibility in melanoma (213). Furthermore, the level of SOCS1 and

SOCS3 activity influence the interferon responsiveness of neuroendocrine tumor cells, and RCL cells, respectively (190, 214).

The PIAS family includes PIAS1, PIAS2, PIASx and PIASy (215). PIAS1 and PIASy are involved in negative regulation of type I IFN signalling (216). Both PIAS1 and PIASy bind to STAT1 and disrupt its DNA binding capability (217, 218). It was observed that over expression of PIASy in mouse embryonic fibroblasts *in vitro* diminished the antiviral activity of IFN-α and IFN-β against VSV, EMCGV, and sendai virus (219).

1. 6.1 Ras signaling

1.6.1.1 The Biology of Ras

The rat sarcoma virus oncogene (Ras) superfamily comprises proteins that share a protein structure that binds to GTP and possesses GTPase activity (220). They switch between two states, an active (GTP bound), and inactive (GDP bound) form (221). This transition is controlled by intrinsic GTPase activity of Ras, guanine nucleotide exchange factor (GEF)s and GTPase activating protein (GAP)s (222, 223). Ras proteins have low intrinsic GTPase activity, such that GEFs and GAPs act in a supplementary manner to increase the rate of exchange and hydrolysis, respectively. GEFs facilitate Ras activation by promoting the release of GDP and exchange for activating GTP, while GAPs facilitate RAS deactivation by promoting GTP hydrolysis to GDP (222, 223). The balance between activation and deactivation is very important for normal functions of Ras (224-226). When activated in the GTP-bound conformation, Ras interacts with many effectors to

control numerous biological responses, including: proliferation, differentiation, cell adhesion, apoptosis, actin cytoskeletal integrity and cell migration (220). Characterized Ras effectors are phosphatidylinositol 3-kinase, Ral guanine nucleotide exchange factors and the Serine/Threonine protein kinase Raf (227, 228).

1.6.1.2 Ras/Raf/MEK pathway

The Ras/Raf/MEK pathway includes a cascade of phosphorylation events performed by members of three key kinase families: serine/threonine protein kinase Raf, mitogen-activated protein/extra cellular signal-regulated kinase (MEK), and Extra cellular Signal-Regulated Kinase (ERK). This pathway can be activated in two ways, one is regulated or physiological activation and the other type is constitutive or oncogenic activation (220).

Physiological activation of the Ras pathways occurs upon activation of receptor tyrosine kinases (RTK) by growth factors and mitogens (Figure 1.5) (225, 226). Appropriate ligand binding is required to activate the RTK, which stimulates the activation of Ras by inducing the GTP-bound state (226). Raf kinase is recruited to the plasma membrane by activated Ras, which leads to phosphorylation and activation of Raf (229). Phosphorylation cascades ensue, where phosphorylated Raf phosphorylates MEK, which phosphorylates and activates ERK (230-232). Activated ERK has a wide variety of targets in the cytoplasm and nucleus including kinases, phosphatases, transcription factors and cytoskeletal proteins.

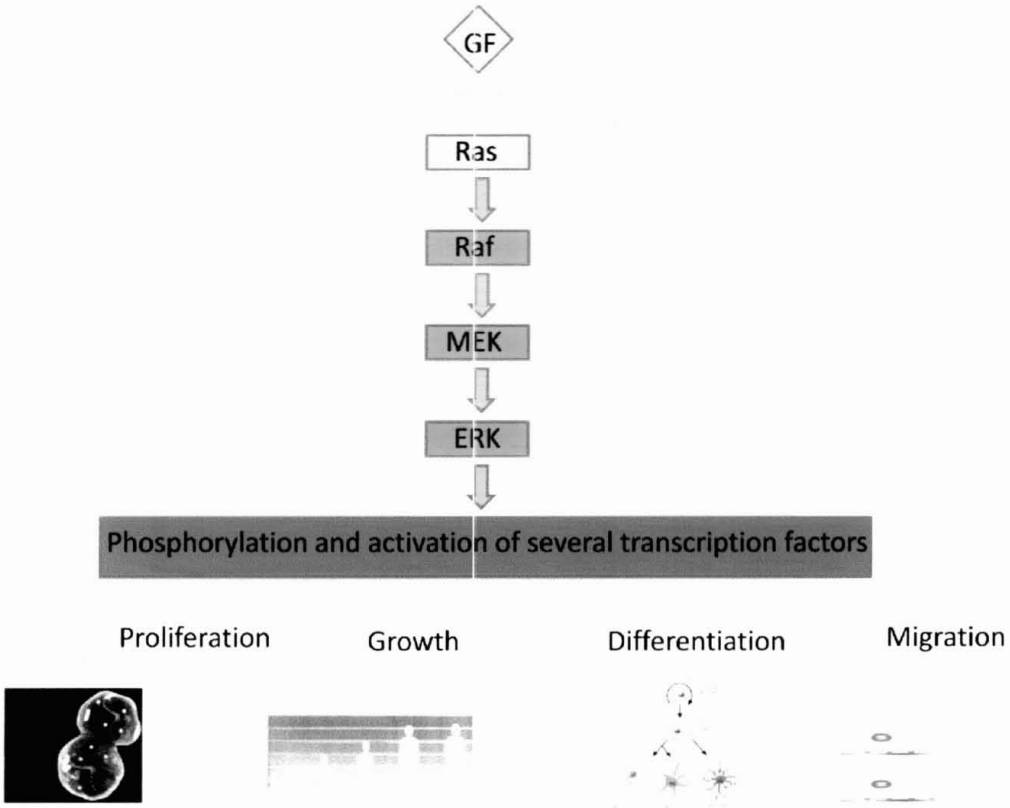

Figure 1.5 Overview of physiological activation of the Ras/Raf/MEK pathway. Following mitogen binding, a phosphorylation cascade starts. This ultimately leads to stimulation of proliferation, growth, differentiation or migration.

The final outcome of physiological activated Ras/Raf/MEK pathway is induction of proliferation, growth, differentiation and migration (233).

Constitutive activation of the Ras/Raf/MEK pathway leads to tumor development, and aberrant activity of this pathway is almost found in one third of all human cancers (224). This type of activation is a consequence of activating mutations in the early components of this pathway including RTKs, Ras, or Raf, or amplification and deregulation of its downstream effectors (220). The outcome is signalling pathway activation that is autonomous from the presence of ligand, and overall loss of regulatory control. The most abundant mutations involved in constitutive activation of Ras are mutations at amino acid residue 12, which represses GAP-mediated inactivation of Ras (234, 235), and mutations in residues 13 and 61 which result in repression of the intrinsic GTPase activity of Ras (234, 235). For pathway components downstream of Ras, B-Raf mutations have been found in many types of malignancies including malignant melanomas, colon cancer, papillary thyroid cancers and serous ovarian cancer (173). Overall, mutations responsible for over-activity of Ras signalling pathway components have been found in 20-25% of all human tumors and up to 90% in specific tumor types such as colorectal cancer (226); therefore, these proteins have been the focus of chemotherapeutic drugs for cancer (236). One of the common Ras/Raf/MEK pathway inhibitors are MEK inhibitors, because MEK is an important regulation step for the pathway (237). Their potential therapeutic benefits have led to developing different types of MEK inhibitors with different structural and chemical properties, in a way that they target different MEKs with different efficiencies (238). Two widely used experimental

inhibitors of MEK 1 and MEK2 are U0126 and SL327. U0126 is used broadly for *in vitro* studies and SL327 for *in vivo* studies (239-241). The obstacles such as not being sufficiently soluble or sufficiently bioavailable and inability of passing blood-brain barriers restricted the *in vivo* application of U0126 (236), resulting in broad application of SL327 *in vivo*, especially for behavioral studies (240-243). Scherle *et al.* applied both U0126 and SL327 in their *in vivo* studies, and identified superiority of SL327 over U0126 for the inhibition of MEK (244).

1.6.1.3 Manipulation of normal Ras/Raf/MEK pathway activity during viral infections

Many viruses evade the host defense system by activating the Ras/Raf/MEK pathway, which is mediated through direct binding of the virus to its receptor or interaction of viral proteins with cellular signalling components. For example, the coxsackie virus induces a biphasic activation of the Ras/Raf/MEK pathway to enhance its protein synthesis and progeny production (244, 245). U0126 treatment of the infected cells significantly decreased viral production and protein synthesis (244, 245). In the early phase of borna virus infection, Ras/Raf/MEK pathway activation facilitates viral propagation, but U0126 treatment reduces the spread of this virus up to 99% (238). Rapid transient activation of the Ras/Raf/MEK pathway also occurs upon respiratory syncytial virus (RSV) infection. Early activation of this pathway plays an important role in RSV-induced early gene expression, since treatment with MEK inhibitor PD98059 resulted in a significant reduction in the RSV infection (246). Furthermore visna virus infection resulted in activation of Ras/Raf/MEK pathway in the early phase of infection, and this

activation remained during all phases of infection. Since PD98059 treatment resulted in a significant reduction of replication, it could be concluded that activation of Ras/Raf/MEK pathway is necessary for visna virus replication (247). As well, activation of Ras/Raf/MEK pathway has been observed for many other viruses such as HIV-1, cytomegalovirus, simian virus, influenza virus, HBV, HCV, and vacina virus (245, 246). Collectively, these reports demonstrate that several viruses use transient activation of Ras/Raf/MEK pathway as a tactic to evade innate immune responses.

1.6.1.4 Exploiting of constitutive Ras/Raf/MEK pathway for promoting oncolytic viruses infection

Many oncolytic viruses preferably replicate in cancer cells harboring constitutive activation of Ras/Raf/MEK pathway to evade innate immune responses and spread their progeny. Examples of those oncolytic viruses are: reovirus (248), adenovirus (249), polivirus (250), HSV (251), VSV (252), and influenza virus (de1NS1 strain) (224). Constitutive Ras/Raf/MEK pathway facilitates viral oncolysis generally through promoting three viral steps, including: uncoating of virus (253, 254), translation of viral proteins (242) and release of new progeny (254, 255).

1.6.1.5 Antagonistic cross talk of the Ras/Raf/MEK pathway and Interferon pathways

Ample evidence shows that manipulation of Ras/Raf/MEK signalling, either in physiological or in constitutive states, is a universal tactic by which different types of

viruses support their own propagation. Our laboratory previously reported that the Ras/Raf/MEK pathway is a cellular suppressor of the type I IFN-induced antiviral response (197). In this study, it was shown that IFN sensitive viruses can infect NIH3T3 cells with activated Ras (RasV12) in the presence of IFN-α, whereas control cells with normal Ras activity were protected from infection by IFN-α. MEK inhibition by chemical inhibitors and knockdown of Ras by RNA interference (RNAi) restored IFN sensitivity in the Ras activated cells. As external validation, Noser *et al.* found that IFN-induced antiviral responses were restored in human cancer cell lines following Ras/Raf/MEK pathway inhibition (256). The evidence puts forward two key points: 1) that viruses benefit from activated Ras signalling to avoid IFN-stimulated immune suppression, and 2) that reversal of Ras activation could sensitize cells to the IFN response.

Experimental efforts to identify IFN signalling components targeted by the Ras/Raf/MEK pathway, revealed reduced total STAT2 protein expression and reduced phosphorylation of STAT2 and STAT1 in RasV12 cells (257). U0126 restored the IFN response completely but re-expression of STAT2 in RasV12 cells resulted in partial recovery of IFN-induced antiviral responses (257). Although STAT2 is recognized as a Ras /Raf/MEK pathways target, evidence such as effective antiviral responses by IFN treatment followed by MEK inhibition, and partial recovery of IFN responses following over expression of STAT2 suggested that Ras/Raf/MEK pathway targets multiple components of IFN signalling, not just STAT2. Therefore, further experiments were performed to determine other elements of the IFN signalling targeted by the Ras/Raf/MEK pathway. Global gene expression profiling by microarray analysis was

conducted to identify the IFN-inducible genes targeted by the Ras/Raf/MEK pathway (Christian, unpublished). NIH3T3 cells transformed with constitutively active Ras (Ras V12) were treated with DMSO (control) IFN-α or U0126. RNA was extracted 6 hrs post treatment and subjected to microarray analysis. Of 41960 gene isoforms represented on the array, 1883 were up-regulated in the Ras V12 cells treated with U0126 compared to control, with a threshold criteria set to a > 2.5 fold increase, while IFN treatment alone induced 1877 genes. Of these candidate genes, 619 were found to be up-regulated by both U0126 and IFN treatment and the group was named MEK-down regulated IFN-inducible genes (MDII genes). Some of the genes were known to have antiviral functions, such as *Gbp2*, *Rig-I*, and *Stat2*. According to microarray analysis data, the U0126 treatment resulted in 9.38 fold increase for *Gbp*2, 2.55 for *Rig-I*, and 6.41 for *Stat2* (Table 1.4). To confirm microarray analysis, the same RNA samples were subjected to quantitative-polymerase chain reaction (q-PCR) for *Gbp2*, *Rig-I*, and *Stat2*. The results from q-PCR analysis showed that MEK inhibition induced the expression of these tested genes significantly and co-treatment of U0126/IFN-α induced synergistic effects (Table 1.4) (Christian; unpublished).

Further experiments were conducted to investigate the influence of the Ras/Raf/MEK pathway on IFN responsiveness in human cancer cell lines, as many

Table 1. 4 MDII genes expression in Rasv12 cells following IFN treatment, MEK inhibition or the combined treatment *in vitro*

GENE	U0126	IFN	U0126/ IFN
Microarray Analysis (RasV12 Cells)			
Gbp2	9.83	97.52	NA
Rig-I	2.55	25.46	NA
Stat2	6.41	16.77	NA
q-PCR Analysis (RaSV12 Cells)			
Gbp2	5.81	78.16	218.51
Rig-I	2.78	20.10	24.64
Stat2	3.74	10.61	24.25

oncolytic viruses exploit pathological activity of this pathway as a mean to replicate in cancer cells (Christian et. al; unpublished). Sixteen cell lines of different origin (3 breast, 1 cervical, 4 colon, 1 fibrosarcoma, 2 melanoma, 3 ovarian and 2 prostate cell lines) were tested for their sensitivity to IFN-α treatment. Three of them were IFN sensitive, 9 of them moderately resistant, and 4 of them were completely resistant. Treatment of U0126 improved the IFN responsiveness in 10 out of 13 moderately and completely resistant cell lines. Further steps were taken to explore the mechanisms which underlie Ras/Raf/MEK pathway mediated IFN resistance in these examined cancer cell lines. Global gene expression profiling by microarray analysis was performed on one IFN sensitive and one moderately IFN resistant cell line treated with DMSO (control), IFN-α or U0126. RNA was extracted 6 hrs and 12 hrs post treatment and subjected to microarray analysis. U0126 treatment increased expression of a group of ISGs such as *Gbp2*, *Rig-I*, and *Stat2*, and these results were confirmed by q-PCR analysis.

Following the observations that the cellular activity of the RAS/Raf/MEK pathway imposed a negative influence on cellular susceptibility to IFN-induced antiviral and antitumor effects via a global down regulation of ISGs *in vitro*, the next step was to assess the physiological application of these findings in an animal model. To our knowledge, this is the first study testing the efficacy of MEK inhibition to promote IFN's transcription activity *in vivo*. It is the ultimate goal of the investigation to explore interventional strategies that improve the efficacy of IFN to cure diseases such as viral infection, MS and cancer.

1.7. HYPOTHESIS AND OBJECTIVES

1.7.1 Hypothesis

MEK inhibition will independently promote the expression of MDII genes, and the co-administration of IFN and a MEK inhibitor will have synergistic effect on MDII gene expression under physiological conditions *in vivo*.

1.7.2 Objectives

1. Investigate whether treatment with a MEK inhibitor promotes expression of representative MDII genes (*Gbp2*, *Rig-I*, *Stat2*) in a mouse model.

2. Investigate whether co-treatment with a MEK inhibitor and IFN-α induces a synergistic effect in the induction of MDII genes (*Gbp2*, *Rig-I*, *Stat2*) in a mouse model.

Chapter 2: Material and Methods

2.1 MICE

Nine week old female mice of the Balb/c inbred strain (Charles River Labs, Boston MA) were used for in vivo experiments. Twenty mice were divided into four groups of five mice receiving the following treatments intraperitoneally (IP): control mice received 80 µl of Dimethylsulfoxide (DMSO) (Sigma, St. Louis MO) plus 120 µl Phosphate Buffered Saline (PBS) (80 g sodium chloride, 2 g potassium chloride, 11.59 g disodium hydrogen phosphate, 2 g/l mono potassium dihydrogen phosphate (Sigma, St. Louis MO)); one group received 100 mg/kg BW of SL327 (Ascent Scientific, Cambridge MA) dissolved in 80 µl of DMSO and then diluted at120 µl; another group received 1000 U IFN-α (Pestka Biomedical Laboratories Interferon Source, Piscataway NJ) dissolved in 100 µl PBS , and one group was co-injected with SL327 (100 mg/kg) and 1000 U IFN-α in their respective vehicles. The mice were sacrificed 8 hrs after injection. The brain, intestine and lungs were harvested to obtain protein samples for western blot analysis and RNA samples for semi-quantitative PCR-based gene expression analysis.

2.2 WESTERN BLOT ANALYSIS

2.2.1 Preparation of protein samples

Tissues were cut into about 50 mg pieces and homogenized in 1 ml of radioimmuno precipitation assay (RIPA) lysis buffer (1X PBS pH 7.4 , 1% nonidet P-40 (Sigma, St. Louis MO), 0.5% sodium deoxycholate (Sigma, St. Louis MO), and 0.2%

sodium dodecyl sulphate (SDS) (USB, Cleveland OH) containing protease and phosphatase inhibitors (100 ng/ml phenyl methyl sulfonyl flouride (Sigma-Aldrich, St. Louis MO), 2 µg/ml leupeptin (Sigma, St. Louis MO), 30 µg/ml aprotinin (Sigma, St. Louis MO), 100 mM sodium vanadate (Sigma, St. Louis MO), and 500 mM sodium fluoride (Sigma, St. Louis MO)). The lysate was centrifuged at 12000 xg for 10 min at 4 °C. Supernatants containing cellular proteins were then separated from debris and kept at -40 °C until the time of assay.

2.2.2 Quantification of protein

The amount of protein was measured with bicinchoninic acid (BCA) Protein assay kit (Pierce Biotechnology Inc., Rockford, IL). BCA reagent (50:1, reagent A: reagent B) was added to 50 µl of protein samples or standards prepared from bovine serum albumin (BSA) (0, 1.0, 1.5, 2.0 and 2.5 µg), and incubated for 30 min at 37 °C. After incubation, absorbance of protein samples was measured with a spectrophotometer (Beckman Coulter , Brea, CA) at 562 nm and the protein concentration of experimental samples determined from the standard curve (Beckman Instruments Inc, Fullerton, CA). After standardizing the protein samples, they were then mixed with 3x bromophenol blue (Sigma, St. Louis MO), boiled at 100 °C for 5 min and stored at -45 °C until the immunoblotting procedure.

2.2.3 Electrophoresis and transfer of proteins

SDS-polyacrylamide gel electrophoresis (SDS-PAGE) was used for separation of protein samples on a 10% separating gel made from: 3.448 ml H_2O, 1.876 ml 1.5 M Tris

(hydroxymethyl) aminomethane-hydrochloride (Tris-HCl), pH 8.8, 2.025 ml 30% acrylamide (29 (Acrylamide) :1 (Bisacrylamide)), 3 µl tetramethylethylenediamine (TEMED) (Bio RAD, Hercules CA), 75 µl 10% ammonium persulfate (APS) (Pharmacia Biotech, Baie-D'Urfé QC). The protein was initially loaded onto a 4.5 % stacking gel: 1.720 ml dH_2O, 760 µl 0.5 M Tris-Hcl pH 6.8, 500 µl 30% acrylamide, 30 µl 10% SDS, 30 µl 10% APS, and 3 µl TEMED. Ten µl/well of each protein samples or pre-stained protein ladder (Benchmark company, New York NY), ranged from10 to 220 kDa, was loaded and then run in mini-protein cell electrophoresis chambers (Bio-Rad, Hercules CA) with gel running buffer (500.2 mM tris base, 38.3 mM glycine (Sigma, St. Louis MO), and 70 mM SDS) at 100 V for 2 hrs. Following electrophoresis, the protein samples were transferred from gels to nitrocellulose membranes (Bio-RAD, Hercules CA) in transfer buffer (20% methanol (ACP, Montreal QC), 39.82 mM glycine, 47.9 mM tris base, 1.28 mM SDS) for 1 h at 100 V.

2.2.4 Immunoblotting

Membranes were blocked with 5% skim milk in tris-buffered saline with tween (20mM tris and 137 mM sodium chloride PH 7.3 containing 0.1% tween 20 (TBST) (Sigma, St. Louis MO) for 1 h, and then incubated with primary antibodies including: anti-phospho-ERK (p-ERK) (1:1000) (Cell Signalling Technology, Danvers MA; Catalog number: 9101) and anti-total-ERK (t-ERK) (1:3000) (Santa Cruz Biotech, Santa Cruz CA; Catalog number: SC94) overnight at 4 °C. The next day they were washed 3 times for 5 min with TBST, and incubated with goat anti-rabbit IgG- horseradish peroxidase (1: 5000) (Santa Cruz Biotech, Santa Cruz CA; Catalog number: K0408) which was used

as the secondary antibody. Following incubation with secondary antibody, membranes were washed 3 times for 5 min with TBST. Bands were visualized on Fuji medical X-ray film (FujiFilm, Tokyo Japan) using AFP imaging developer (AFP Imaging Corp, Elmsford NY) following incubation of the membranes with millipore chemiluminescent detection kit (Millipore, Billerica MA). The band images were scanned using an epson perfection 3170 photo scanner (Epson, Tokyo Japan) to get the image in digital format for subsequent densitometry analysis.

2. 3. RT-PCR

2.3.1 RNA Extraction

RNA was extracted with TRIzol (Invitrogen, Burlington ON) according to the manufacturer's instruction. RNA extraction consists of five procedures: homogenization, separation, precipitation, RNA wash, and re-dissolving the RNA. At the homogenization step, tissue samples with about 50 mg weight were homogenized in 1ml of TRIzol applying a glass-Teflon homogenizer. At the separation phase homogenized samples were incubated for 5 min at room temperature, and then 0.2ml of chloroform (Sigma, St. Louis MO) was added to samples. Tubes were shaken vigorously by hand for 15 sec and incubated at room temperature for 3 min. Next, samples were centrifuged at 12000 xg for 15 min at 4 °C. After centrifuge, the aqueous phase, which contained RNA was separated and placed in new tubes, and the organic phase was kept for future DNA and protein extraction. To precipitate RNA from aqueous phase, 0.5 ml isopropanol (Sigma, St. Louis MO) was added to each tube, and then the mixture was incubated at room temperature for

10 min. After incubation, samples were centrifuged at 12000 xg for 10 min at 4 °C. At the washing level, supernatant was removed, and 1 ml ethanol 75% (Sigma, St. Louis MO) was added to each pallet. The mixture was then vortexed and centrifuged at 7500 xg for 5 min at 4 °C. At the re-dissolving step, samples were air dried after centrifuge for 10 min. pallet was then dissolved at RNAase-free water, followed by incubating the mixture for 10 min at 60 °C. The quantity and quality of samples were measured based on 260/280 nm ratios by Nanodrop 1000 spectrophotometer (Thermo Scientific, Waltham MA).

2. 3.2 cDNA Synthesis

Complementary DNA (cDNA) was synthesized using RevertAid™ H Minus first strand cDNA synthesis kit (Fermentas, Burlington ON). The RT mixture included: RevertAid™ H Minus M-MuLV reverse transcriptase, 5X reaction buffer, Ribolock RNase inhibitor, 10 mM dNTP mix, random hexamer primer, and 500 ng RNA diluted in a total volume of 6 µl Diethylpyrocarbonate-treated water. Samples were incubated for 5 min at 25 °C followed by 60 min at 42 °C. The reaction was terminated by heating at 70 °C for 5 min.

2.3.3 Standard PCR

The expression levels of *Gapdh*, *Gbp2*, *Rig-I* and *Stat2* mRNA were measured following limited PCR amplification using gene-specific oligonucleotide primers described in (Table 2.1). The PCR reaction mixture included: 2 µl 10X buffer, 1 µl MgCl2,

Table 2.1 Gene specific primer sequences

Gene	Primer forward	Primer reverse	size bp
Gapdh	5'-GGG TGG AGC CAA ACG GGT CA-3'	5'-GGA GGT GCT GTT GAA GTC GCA-3'	532
Gbp2	5'- AGGTTAACGGAAAACCCGTCA-3'	5'- CACAGTCGCGGCTCATTAAAG-3'	106
Rig-I	5'- GGCAGACAAAGAGGAGGAGA-3'	5'- CGGACATCGTGGAAGAAGG-3'	150
Stat2	5'-GTC TTC AGA CCC CCA TCA GA-3'	5-CTG CCT TCC TGG AGT CTC AC-3'	507

(Fermentas, Burlington ON), 0.2 µl 10 mM deoxynucleotide triphosphate mix (dNTP), 0.2µl Taq polymerase (Invitrogen, Burlington ON) ,0.5 µl of 10 mM forward primer, 0.5 µl of 10 mM reverse primer (Integrated DNA Technologies, Coralville IA) and 14.6 µl distilled water. The PCR reaction was carried out as follows: denaturation at 94 °C for 1 min, annealing at 63.5 °C for 1 min, extension at 72 °C for 1 min for 32 cycles for *Gbp2*, *Rig-I*, and Stat2. The annealing temperature was set at 63 °C for *Gapdh* and proceeded for only 29 cycles of amplification. The final extension was carried out at 72 °C for 10 min for all the reactions.

2.3.4 Electrophoresis of PCR products

Five µl of the PCR products mixed with 0.5 µl of loading buffer as well as 3 µl of 100 bp ladder (Fermentas, Burlington ON) were run on 1% Agarose gel (Invitrogen, Burlington ON) containing Ethidium Bromide (Invitrogen, Burlington ON) placed on a horizontal gel transfer apparatus for 30 min. The gel transfer apparatus was filled with 1x Tris acetate (50x stock/ml: 242 g tris base, 57.1 ml glocial acetic acid, 100 ml PH.8 0.5 m ethylene diamine tetra acetic acid). The PCR products were observed under UV light using a gel logic 200 imaging system (Eastman Kodak Company, New York NY).

2.4 DENSITOMETRY ANALYSIS

Densitometry analysis on scanned protein films and Ethidium stained gels was performed with Image J software (NIH, Bethesda, Maryland, USA,

http://imagej.nih.gov/ij/). Protein bands were normalized to t-ERK and RT-PCR bands were normalized to *Gapdh*.

2.5 STATISTICAL ANALYSIS

Statistical analysis of the protein and RT-PCR densitometry ratios was performed using One-way Analysis of Variance (ANOVA) by GraphPad Prism Version 4 (GraphPad Software, La Jolla California USA).

Chapter 3: Results

3.1. EFFICACY OF SL327 TREATMENT ON INHIBITION OF Ras/Raf/MEK PATHWAY IN VIVO

The first step of the experimental strategy was to determine whether the MEK inhibitor SL327 can inhibit the activity of the Ras/Raf/MEK pathway *in vivo*. Western blot analysis was performed to examine the activation state of ERK kinase, the downstream target of MEK, and this was represented by the phosphorylation status of ERK (p-ERK). p-ERK was examined in protein lysates prepared from the lungs of three mice injected intraperitoneally with DMSO or SL327 in DMSO (100 mg/kg BW). A specific antibody against p-ERK was used to assess the phosphorylation state, as an indicator for the efficacy of the SL327 treatment. Intraperitoneal injection of SL327 reduced the relative ratio of phosphorylated to t-ERK in the lungs (Figure 3.1 and Figure 3.2). The same dose and site of drug administration was used for subsequent experiments.

3.2. EFFECTS OF PHYSIOLOGICAL LEVELS OF ACTIVE Ras/Raf/MEK PATHWAY ON EXPRESSION LEVELS OF MDII GENES IN THE BRAIN, INTESTINE, AND LUNG

If the physiological activation of the Ras/Raf/MEK pathway suppresses the expression of the MDII genes, inhibition of Ras/Raf/MEK would be expected to increase their expression.

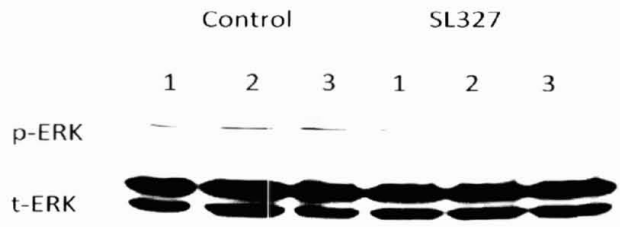

Figure 3.1 Western blot analysis of p-ERK in the lung. Mice were injected intraperitoneally with 80 µl of DMSO (control) or SL327 (100 mg/Kg). At 8 hrs after injection, protein samples were prepared from the lungs for western blot analysis. The membranes were blotted with antibodies against p-ERK, and t-ERK. Each lane number represents an individual mouse per treatment.

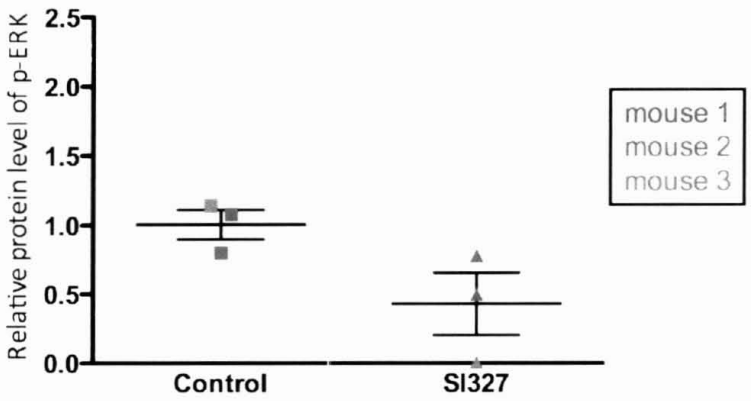

Figure 3.2 Densitometry analysis of p-ERK in the lung. Protein samples were prepared from the lungs of mice intraperitoneally injected with 80 µl of DMSO (control) or SL327 (100 mg/Kg). Following western blotting, densitometry of the bands was measured with NIH Image J. The band density of p-ERK was normalized to that of t-ERK and plotted per mouse. Horizontal lines represent the mean density ± SEM.

To examine this hypothesis, Balb/c female mice were treated with DMSO (control, n=5), 100 mg/kg SL327 (n=5), 1000 U/mouse IFN-α (n=5), or the combination of IFN-α/ SL327 (n=5). RNA was extracted from the brain, lung, and intestine at 8 hrs post injection and subjected to semi-quantitative RT-PCR to measure the expression of the MDII genes: *Gbp2*, *Rig-I* and *Stat2*.

3.2.1 Brain

Figure 3.3 shows the relative changes in electrophoresis banding patterns for the MDII genes in the brain of mice that received control DMSO injection, SL327 alone, IFN-α alone or SL327 in combination with IFN-α. In Figure 3.4, the densitometric ratios for *Gbp2*, *Rig-I* and *Stat2* relative to *Gapdh* are plotted for individual mice across the four different treatment groups, along with the mean expression change.

IFN-α treatment induced expression of *Gbp2* in all individual mice, but the individual mouse responses were quite variable in SL327 treatment group (Figure 3.3 A). For example, mouse 1 and 2 were the only responders to SL327 treatment based on this semi-quantitative analysis. As a group, there were no significant changes in *Gbp2* relative expression relative to mice receiving the vehicle control in the brain (Figure 3.4A). Co-injection of IFN-α and SL327 induced no synergistic effect (Figure 3.3 A, Figure 3.4 A).

The individual mouse responses were quite variable for *Rig-I* expression in the brain of IFN-α treatment groups (Figure 3.3 B). For example: most robust induction of *Rig-I* was observed in mouse 3, 4, and 5, as the induction in mouse 1, and 2 was not considerable.

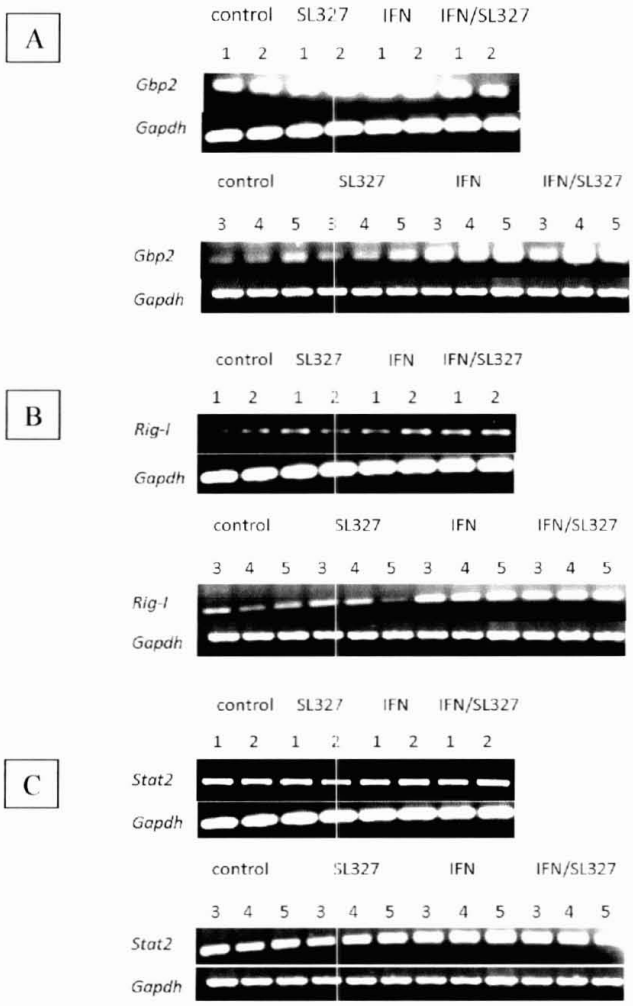

Figure 3.3 RT-PCR analysis of the brain samples. RNA was extracted from the brain of animals treated with DMSO (cont, n=5), and 100 mg/Kg SL327 (n=5), 1000 U/mouse IFN-α (n=5), and SL327/IFN-α (n=5), at 8 hrs after injection. RT-PCR analysis was performed for *Gbp2*, *Rig-I*, *Stat2*, and *Gapdh*. Each number represents an individual mouse per treatment.

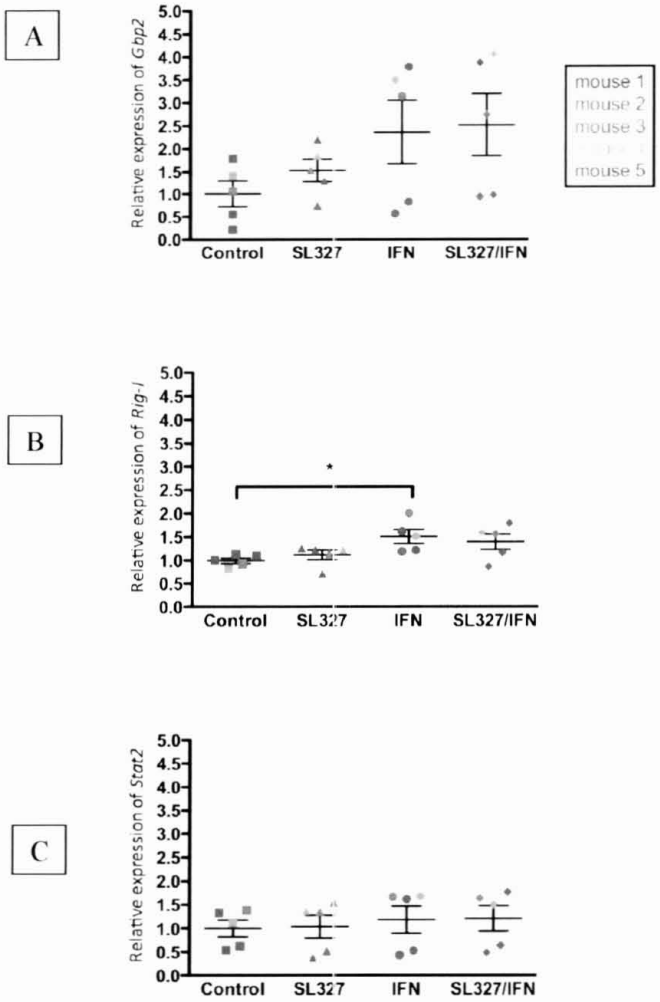

Figure 3.4 Densitometry analysis of the RT-PCR results of the brain samples. RNA was extracted from the brain of animals treated with DMSO (cont, n=5), and 100 mg/Kg SL327 (n=5), 1000 U/mouse IFN-α (n=5), and SL327/IFN-α (n=5), at 8 hrs after injection. The band intensity of MDII genes was normalized to that of *Gapdh* and plotted per mouse. * $P< 0.05$ by one-way analysis of Variance (ANOVA). Horizontal lines represent the mean density ± SEM.

Expression of *Rig-I* was up-regulated in none of the mice following SL327 administration. As a group, there were only significant changes in *Rig-I* relative expression in the IFN-α treatment group relative to mice receiving the vehicle control (Figure 3.4 B). Co-injection of IFN-α and SL327 induced no synergistic effect (Figure 3.3 B; Figure 3.4 B).

Similarly, individual mouse responses were quite variable for *Stat2* expression in the brain of all treatment groups (Figure 3.3 C). For example: mouse 1 and 2 were non-responders to any treatment based on this RT-PCR analysis. Mouse 3, 4 and 5 showed an up-regulation of *Stat2* expression in the brain following IFN-α, but only in mouse 5 *Stat2* expression was induced following SL327 treatment. As a group, there were no significant changes in *Stat2* relative expression in the brain compared to mice receiving the vehicle control (Figure 3.4 C). Co-injection of IFN-α and SL327 induced no synergistic effect (Figure 3.3 C; Figure 3.4 C).

3.2.2 Intestine

Figure 3.5 shows the relative changes in electrophoresis banding patterns for MDII genes in the intestine of mice that received control DMSO injection, SL327 alone, IFN-α alone or SL327 in combination with IFN-α. In Figure 3.6, the densitometric ratios for *Gbp2*, *Rig-I* and *Stat2* relative to *Gapdh* are plotted for individual mice across the four different treatment groups, along with the mean expression change.

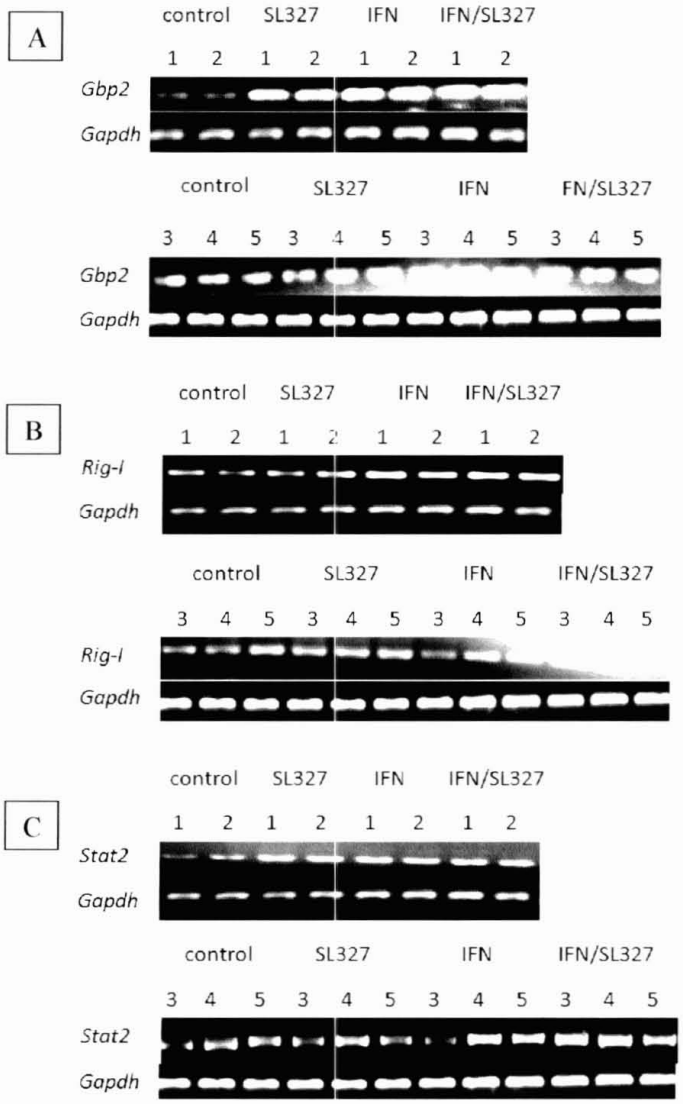

Figure 3.5 RT-PCR analyses of the intestine samples. RNA was extracted from the intestine of animals treated with DMSO (cont, n=5), and 100 mg/Kg SL327 (n=5), 1000 U/mouse IFN-α (n=5), and SL327/IFN-α (n=5), at 8 hrs after injection. RT-PCR analysis was performed for *Gbp2*, *Rig-I*, *Stat2*, and *Gapdh*. Each number represents an individual mouse per treatment.

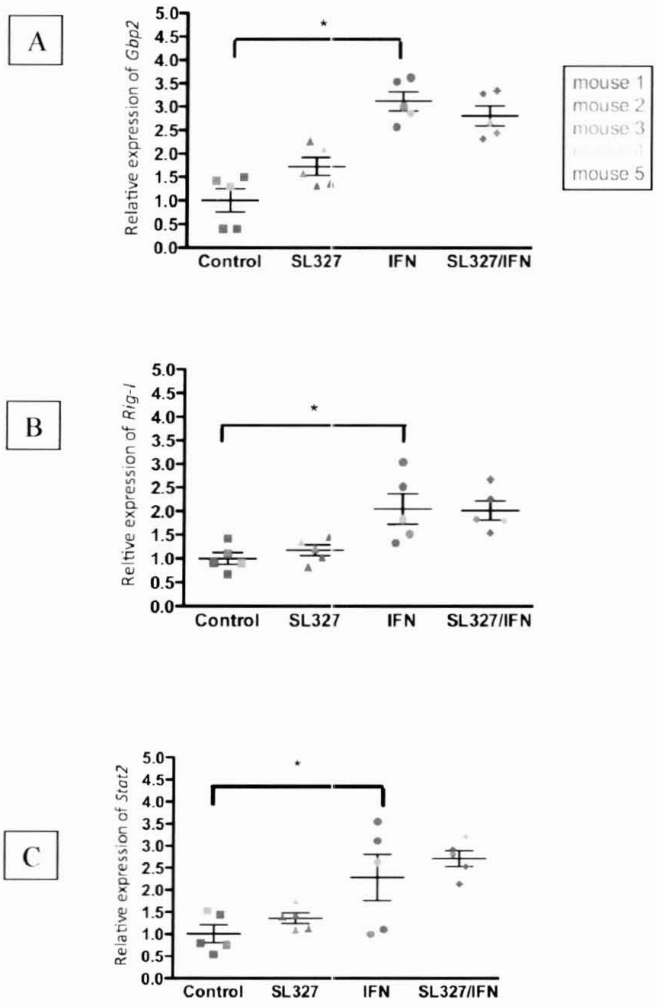

Figure 3.6 Densitometry analysis of the RT-PCR results of the intestine samples.

RNA was extracted from the intestine of animals treated with DMSO (cont, n=5), and 100 mg/Kg SL327 (n=5), 1000 U/mouse IFN-α (n=5), and SL327/IFN-α (n=5), at 8 hrs after injection .The band intensity of MDII genes were normalized to that of *Gapdh* and plotted per mouse. * $P< 0.05$ by one-way analysis of Variance (ANOVA). Horizontal lines represent the mean density ± SEM.

All mice showed an up-regulation of *Gbp2* expression in the intestine following IFN-α administration (Figure 3.5 A). The individual mouse responses were variable for *Gbp2* in the intestine of SL327 treatment groups, as despite mouse 1, 2, 3, 4, and 5, mouse 3 showed no induction of this gene (Figure 3.5 A). As a group, there were only significant changes in *Gbp2* relative expression in IFN-α treated group relative to mice receiving the vehicle control (Figure 3.6 A). Co-injection of IFN-α and SL327 induced no synergistic effect (Figure 3.5 A; Figure 3.6 A).

IFN-α treatment induced expression of *Rig-I* in the intestine of all individual mice, with a more robust induction in mouse 1 and 2 (Figure 3.5 B). SL327 induced no changes in expression level of *Rig-I* in the intestine of any individual mice (Figure 3.5 B). Grouping the responses of all five mice per treatment group, there was only significant changes in *Rig-I* relative expression in IFN-α treated group relative to mice receiving the vehicle control (Figure 3.6 B). Co-injection of IFN-α and SL327 induced no synergistic effect (Figure 3.5 B; Figure 3.6 B).

The individual mouse responses were variable for *Stat2* expression in the intestine of all treatment groups; for example, mouse 3 did not respond to IFN-α treatment (Figure 3.5 C). SL327 increased expression of *Stat2* only in intestine of mouse 1 and 2 (Figure 3.5 C). As a group, there were only significant changes in *Stat2* relative expression in IFN-α treated group relative to mice receiving the vehicle control (Figure 3.6 C). Co-injection of IFN-α and SL327 induced no synergistic effect (Figure 3.5 C; Figure 3.6 C).

3.2.3 Lung

Figure 3.7 shows the relative changes in electrophoresis banding patterns for the MDII genes in the lung of female mice that received control DMSO injection, SL327 alone, IFN-α alone or SL327 in combination with IFN-α. In Figure 3.8, the densitometric ratios for *Gbp2*, *Rig-I* and *Stat2* relative to *Gapdh* are plotted for individual mice across the four different treatment groups, along with the mean expression change.

The individual mouse responses were variable for *Gbp2* expression in the lung of IFN-α treatment groups, with mouse 3, 4, and 5 showing a relatively robust response, but mouse 1 and 2 were non-responders to IFN-α treatment based on the *Gbp2* profile (Figure 3.7 A). All mice showed an up-regulation of *Gbp2* expression in the intestine following SL327 administration (Figure 3.7 A). As a group, there were no significant changes in *Gbp2* relative expression in the lung compared to mice receiving the vehicle control (Figure 3.8 A). Co- injection of IFN-α and SL327 induced no synergistic effect (Figure 3.7 A; Figure 3.8 A).

The individual mouse responses were quite variable for *Rig-I* expression in the lung of all treatment groups, for example, as only mouse 1 and 2 were responders to IFN-α or SL327 treatment based on this RT-PCR analysis (Figure 3.7 B). As a group, there were no significant changes in *Rig-I* relative expression relative to mice receiving the vehicle control (Figure 3.8 B). Co- injection of IFN-α and SL327 induced no synergistic effect (Figure 3.7 B; Figure 3.8 B).

All mice showed an up-regulation of *Stat2* expression in the lung following IFN-α administration (Figure 3.7 C). The individual mouse responses were quite variable for

SL327 treatment group, as only mouse 1 and 2 were responder to this treatment (Figure 3.7 C). As a group, there were no significant changes in *Stat2* relative expression relative to mice receiving the vehicle control (Figure 3.8 C). Co-injection of IFN-α and SL327 induced no synergistic effect (Figure 3.7 C; Figure 3.8 C).

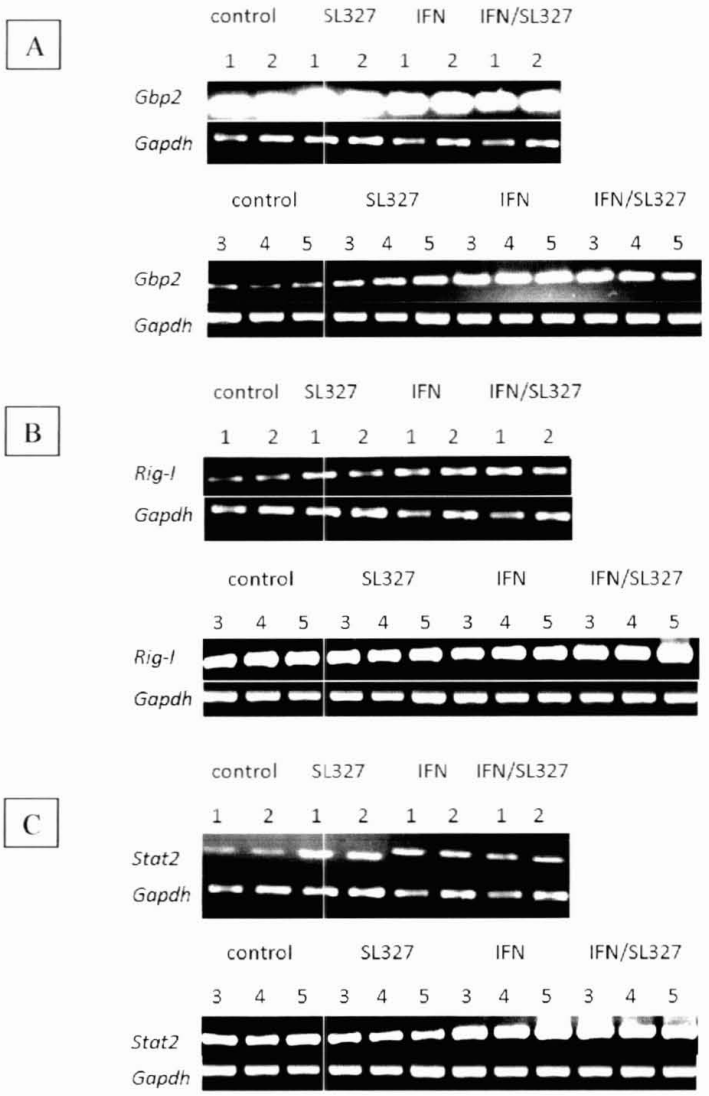

Figure3. 7 RT-PCR analyses of the lung samples. RNA was extracted from the lung of animals treated with DMSO (cont, n=5), and 100 mg/Kg SL327 (n=5), 1000 U/mouse IFN-α (n=5), and SL327/IFN-α (n=5), at 8 hrs after injection. RT-PCR analysis was performed for *Gbp2*, *Rig-I*, *Stat2*, and *Gapdh*. Each number represents an individual mouse per treatment.

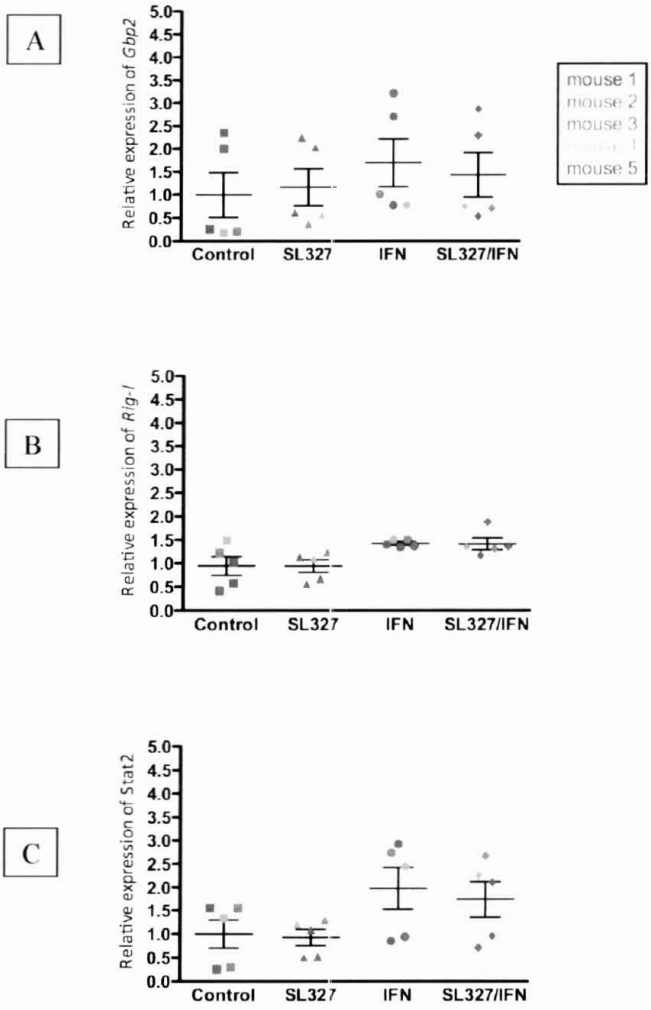

Figure 3.8 Densitometry analysis of the RT-PCR results of the lung samples. RNA was extracted from the lung of animals treated with DMSO (cont, n=5), and 100 mg/Kg SL327 (n=5), 1000 U/mouse IFN-α (n=5), and SL327/IFN-α (n=5), at 8 hrs after injection. The band intensity of MDII genes were normalized to that of *Gapdh* and plotted per each individual mice. * $P< 0.05$ by one-way analysis of Variance (ANOVA). Horizontal lines represent the mean density ± SEM.

Chapter 4: Discussion

4.1 APPLICATION OF MEK INHIBITORS AS A STRATEGY TO PROMOTE IFN EFFICACY

Type I IFNs have been approved as a therapeutic agent for various pathological conditions, such as: HCV, HBV, HIV, HCL, CML, certain types of B- and T-cell lymphoma, melanoma, renal cell carcinoma and MS (1, 2). Even though other targeted therapies have replaced type I IFNs as the primary treatment strategy for some of these conditions, they are still an important therapy option for HBV, HCV, melanoma and MS, either alone or in combination with other therapies (150, 151, 172, 179). Unfortunately, despite high expectations for the therapeutic benefits of IFN therapy, the rate of response is limited by an inherent or acquired IFN resistance phenotype in non-responsive patients (187). One of the main contributors to poor therapeutic outcome is deregulation and over-activity of endogenous cellular suppressors of IFN signalling (210, 211, 256). Ongoing investigations are focussed on the potential to target the endogenous cellular suppressors to improve IFN responsiveness (205, 213, 214). For instance, due to promising combination effects of IFN-α with an inhibitor of SHP1 phosphatase-sodium stibogluconate, using *in vitro* and *in vivo* model systems, clinical trials have progressed to phase I for the combination treatment of melanoma (206).

Our laboratory has identified the Ras/Raf/MEK pathway as an endogenous inhibitor of type I IFN signalling (197, 257). Activation of the Ras/Raf/MEK pathway triggers diminished IFN-α-induced antiviral and antitumor responses that are mediated through global down-regulation of ISGs in a cell model (197, 257) (Chrisian et al

unpublished). Conversely, inhibition of Ras/Raf/MEK pathway via MEK inhibitor U0126 *in vitro* induced a profound reversal in the IFN-α responsiveness, and synergistic up-regulation of ISGs when co-applied with IFN-α (197, 257) (Christian et al unpublished). These observations shaped the hypothesis of my research thesis, to explore the therapeutic value of co-application of IFN-α and a MEK inhibitor in a mouse model. This study was a first step towards improved type I IFN therapy based on Ras/Raf/MEK pathway targeting.

4.2 EFFECTS OF IFN-α AND SL327 COMBINATIONS ON MDII GENES EXPRESSION

The IFN treated groups were a positive control for evaluating the accuracy of the experimental procedures. Significant induction of all tested genes by IFN-α in the intestine, and significant induction of the *Rig-I* in the brain suggests that the experimental procedures including RNA extraction, PCR, densitometry and statistical analysis were properly performed.

Western blot analysis using anti-p-ERK antibody revealed that SL327 successfully inhibited Ras/Raf/MEK pathway. Even though the degree of inhibition was correlated with up-regulation of MDII genes in some individual mice, it did not have a statistically significant effect on the overall mean of SL327 treated group compared to the control group for none of the genes in any organs. IFN-α/SL327 co-injection also induced no additive or synergistic effect. These outcomes are very different from prior *in vitro* results, where MEK inhibition significantly restored the expression of MDII genes with determinant roles in type I IFN signalling such as *Gbp2*, *Rig-I*, and *Stat2*. In this research, MEK inhibition followed by 1.5-1.75 fold changes for *Gbp2*, 1-1.2 fold changes for *Rig-I*,

and 1-1.2 fold changes for *Stat2*, while the relevant ratio measure from the *in vitro* studies were 5.8-9.83 fold changes for *Gbp2*, 2.55- 2.78 fold changes for *Rig-I*, and 3.74-6.41 fold changes for *Stat2*. This discrepancy between *in vitro* and *in vivo* observations might be explained by several factors including: different experimental design between the two studies (cellular vs animal model), time and concentration dependence of drugs and observed degree of variation between individual mice.

4.3 EXPRIMENTAL DESIGN: IN VITRO VS IN VIVO

The *in vivo* experiments explored in this work were designed based on literature reports and empirical data gathered from cell models for MEK inhibition and type I IFN signalling response in the Hirasawa lab. There were several methodological differences between the *in vitro* and *in vivo* studies: 1) change of model of study from cell culture to animal; 2) change of measurement strategy from q-PCR to RT-PCR; and 3) change of MEK inhibitor from U0126 to SL327.

Recognition that the oncogenic activity of the Ras/Raf/MEK pathway determined cellular type I IFN susceptibility *in vitro*, the logical step was to determine the physiological application of these findings. This was important because, as discussed in section 1.6.1.3, many viruses exploit physiological activation of Ras/Raf/MEK pathway for their replication. Inbred female mice that were not virally, immunologically or tumor-challenged were chosen as a model to investigate influence of physiological activation of Ras/Raf/MEK pathway on type I IFN responsiveness. Animal models are more complex than cell culture, and results can be variable based on different conditions. Pharmacokinetics is very different from a culture model where each cell receives the

same drug dose in the medium relative to cells distributed in tissues and organs of intact animals. In addition, drugs administrated *in vivo* can be injected into different parts of the animal's body, which may produce different results. In this study, the most robust induction of IFN-α response occurred in the intestine and a question raises here is that whether the significant stimulation of IFN-α response in intestine is an influence of route of injection?

Another complexity of working with mouse model is the genetic difference between various strains of mice, such that changing the strain of mice may lead to different results. For example, in efforts for learning about RIG-I functions, in one study conducted in C57BL/6 female mice, knock down of *Rig-I* was lethal (42), but in another independent study, *Rig-I* deficient mice, obtained from intercrossing of C57BL/6 female mice with ICR mice, were viable (49). In addition, Groblewski *et al.* were exploring the effect of ERK signalling, applying SL327 on some aspects of ethanol seeking behaviour in male DBA/ 2J mice but they found no correlation (240). Their findings were in contrast with two other independent studies (258, 259), and they discussed differences in mice strains as one of the main reasons of the inconsistency (240). Like individuals that have different sensitivity to IFNs, different strains of mice might have different sensitivity to drugs applied in this study. We ran a proof-of- principle experiment, and this demands a sensitive and thorough design. In this regard, first, it is logical to obtain an estimate of response in normal cells, independent of variables such as strain of mice and route of injection, and this would inform the next round of mouse studies.

The expressional changes were detected by q-PCR *in vitro*, while RT-PCR was applied *in vivo*. Since several viruses exploit physiological activation of Ras/Raf/MEK

pathway to spread their progeny, we expected that similar to its constitutive form of activity, normal activity of this signalling pathway would have considerable effects on IFN responsiveness. Therefore, we speculated that RT-PCR is sensitive enough to detect those major changes. This technique was also was used by Klampfer *et al.* while they were investigating the effect of oncogenic Ki-Ras on type II IFN responsiveness (260). Results of my study showed less than 2 fold changes of all tested MDII genes, while relevant rates from *in vitro* studies were more than two fold (Table 1.4). My results raise two questions: whether inhibition of physiological activation of Ras/Raf/MEK pathway is adequate for significant induction of MDII genes expression, and whether RT-PCR methodology is sensitive enough to detect these changes. These questions will be tested in future *in vitro* studies, as the answer is very important for designing the next round of mouse studies.

Another difference between the two studies was a transition from U0126 to SL327 treatment. Type of MEK inhibitor is a variable, which may have influenced the results of my experiments (238). However, Christian *et al.* found no significant difference between the efficacy of SL327 and U0126 *in vitro* (257). In addition, Scherle *et al.* and others reported superiority of SL327 over U0126 for *in vivo* studies (244). My results also confirmed down-regulation of p-ERK by SL327 *in vivo*. Therefore, it is not expected that switching from U0126 to SL327 led to inconsistency between two investigations.

4.4 TIME AND DOSE DEPENDENCY OF MEK INHIBITORS AND TYPE I IFNs

Based on the literature, both MEK inhibitors and type I IFNs, similar to most drugs, are time and concentration dependent (240, 241, 261, 262). Accordingly, restoration of IFN-α response by MEK inhibition was proven within a range of time

points (0-24 hrs) and U0126 doses (1.25-20 μM) during former studies in our laboratory (197, 257). As a start for performing an *in vivo* pilot study, one time point (8 hrs) and concentration (100 mg/kg) based on former preliminary data and maximum dose tolerance of animals was selected.

Induction of ISGs can occur in two phases, including: primary response which happens within minutes of post injection without need for new protein synthesis; secondary responses which happen within hours post injection and require new protein synthesis (85). Depending on the experimental conditions, investigations focusing on gene expressional analysis of ISGs are usually conducted between 30 min and up to 48 hrs of post injection (13, 261-264). Former studies in our laboratory identified that the most robust stimulatory effect of MEK inhibition on ISGs transcription was at 6 hrs post stimulation (197, 257) (Christian *et al.* unpublished). Since *in vivo* is more complex than *in vitro*, we anticipated that it may take longer for MEK inhibitor to effectively inhibit Ras/Raf/MEK pathway *in vivo*, thereby 8 hrs was chosen as a time point of this study. Future *in vivo* studies should be performed with testing more time points testing either before or after 8 hrs.

Expressional analysis of type I IFN signalling in normal conditions is usually within a concentration range of 100 IU- 1000 IU (13, 264), while the related range for SL327 is between 25 mg/kg-100 mg/kg (240-243). Toxicity tests in Hirasawa laboratory revealed a dosage limit of 100 mg/kg for SL327 and 1000 IU for IFN-α. Therefore, aiming to obtain the most robust induction, we followed a general theme, which was applying highest allowed dosage, but induction levels were not as high as we expected. This does not mean that there is no logic of trying lower dosages, especially when we are

seeking to observing synergistic effect. The hypothesis of my thesis was tested in normal mice; therefore, high dose of IFN-α may mask synergistic effect. Groblewski *et al.*, during their investigations on understanding the effects of ERK signalling on ethanol seeking behaviour, applied two doses of SL327, including: 30 mg/kg and 50 mg/kg (240). They observed the reverse effect for 50 mg/kg, but not with 30 mg/kg. This suggests that applying high dosages of SL327 may not be always suitable. In addition, Yi *et al.* conducted dosage course experiments to evaluate potential synergistic effect of IFN-α with an inhibitor of SHP1 and SHP2 inhibitor sodium stibogluconate (204). They combined 1000 IU of IFN-α with different dosages of sodium stibogluconate ranging from 25-200 μg/ml, and the most robust synergistic effect was observed in the treatment of 25 μg/ml sodium stibogluconate (204). Altogether, future studies should be expanded with different sets of experiments testing a range of dosages: 1) experimental setting 1: use one dosage of IFN mixing with different dosages of MEK inhibitor; 2) experimental setting 2: use one dosage of MEK inhibitor combining with different dosages of IFN; 3) using data from experimental setting 1 and 2 and testing several dosages of SL327 and IFN together. These studies will help us in finding the best dosage for obtaining the most robust induction and synergistic effect.

4.5 MODEL SYSTEM VARIABILITY

High level of variation compromises the power of a statistical test to find significant difference, while the greater number of samples provides a better estimation of the variation to be expected in the response (265). The results of this study suggested that a high degree of variation is to be expected, based on the semi-quantitative gene

expression analysis. Therefore, a set of five animals per treatment is likely an underestimate of the number of animals required to come to a firm conclusion. To avoid false negative conclusions, the next round of mouse studies should be expanded with more mice and a statistical power calculation.

4.6 CONCLUSION

This was a pilot study to contribute to the advancement of practical strategies for improvement of type I IFN therapy. We investigated the influence of co-administration of a MEK inhibitor with IFN-α for the expression of ISG (MDII) genes under physiological conditions *in vivo*. Although in the current study we did not observe the significant effect of MEK inhibition on IFN-α responsiveness either in the absence or presence of exogenous IFN-α, it remains possible that other cell types under different conditions may yield different results. Therefore, it is important to consider developing new animal and cell-based models to define specific means to improve IFN-α sensitivity. This exploration might require a broader array of mouse models, such as genetically engineered strains that are models of cancer, autoimmune disease or that show enhanced sensitivity to viral infection.

4.7 FUTURE DIRECTIONS

1. Conducting *in vitro* experiments to determine the effect of the Ras/Raf/MEK pathway on IFN-α responsiveness in normal cell lines without constitutive Ras/Raf/MEK activation.

Animal studies are very challenging and expensive, and results can be variable based on different parameters such as route of injection, genotype of mouse, number of individuals. *In vitro* studies help to get an estimation of relation of these two signalling pathways excluding the effects of variable parameters. A normal cell line such as NIH3T3 will be chosen as a model of study, and will be treated with a MEK inhibitor, IFN-α and a combination of both. Protein and gene expression analysis will perform to seek outcomes. These sets of experiments will be performed with several time points, concentrations, and several common *in vivo* MEK inhibitors. In addition, expressional analysis will be performed by applying both q-PCR and RT-PCR. This multistep analysis will help with better designing of the next round of mouse studies.

2. Conducting a new round of *in vivo* studies to develop strategies to improve type I IFN therapy by targeting Ras/Raf/MEK.

These set of experiments will be designed if significant results are observed from two *in vitro* experiments. *In vivo* experiments will be conducted in mouse models challenged with viral infection, harboring MS or cancer. These models will be treated with MEK inhibitor, IFN-α and a combination of both. Experiments will be run with a greater number of individuals (>10) and testing several time points and concentrations. The disease progression will be assessed to determine the efficacy of MEK inhibition on improving the type I IFN therapy outcome.

Bibliography

1. Pfeffer LM, Dinarello CA, Herberman RB, Williams BR, Borden EC, Bordens R, et al. Biological properties of recombinant alpha-interferons: 40th anniversary of the discovery of interferons. Cancer Research. 1998 Jun 15;58(12):2489-99.

2. Borden EC, Sen GC, Uze G, Silverman RH, Ransohoff RM, Foster GR, et al. Interferons at age 50: past, current and future impact on biomedicine. Nature Reviews Drug discovery. 2007;6(12):975-90.

3. Lindenmann J. Induction of chick interferon: Procedures of the original experiments. Methods in Enzymology. 1981;78:181-8.

4. Billiau A. Interferon: The pathways of discovery: I. Molecular and cellular aspects. Cytokine & Growth Factor Reviews. 2006;17(5):381-409.

5. Merigan TC. Purified interferons: Physical properties and species specificity. Science. 1964;145(3634):811-3.

6. Pestka S, Krause CD, Walter MR. Interferons, interferon-like cytokines, and their receptors. Immunological Reviews. 2004;202(1):8-32.

7. Levy WP, Rubinstein M, Shively J, Del Valle U, Lai CY, Moschera J, et al. Amino acid sequence of a human leukocyte interferon. Proceedings of the National Academy of Sciences. 1981;78(10):6186.

8. Foster GR. Past, Present, and Future Hepatitis C Treatments. Semin Liver Dis. 2004 02.09.2004;24(S 2):97,104.

9. Hoofnagle JH, Peters M, Mullen KD, Jones DB, Rustgi V, Di Bisceglie A, et al. Randomized, controlled trial of recombinant human alpha-interferon in patients with chronic hepatitis B. Gastroenterology. 1988;95(5):1318.

10. Pasquali S, Mocellin S. The anticancer face of Interferon alpha (IFN-Alpha): From biology to clinical results, with a focus on melanoma. Current Medicinal Chemistry. 2010;17(29):3327-36.

11. Talpaz M, editor. Interferon-alfa-based treatment of chronic myeloid leukemia and implications of signal transduction inhibition2001: Elsevier.

12. Knobler R, Panitch H, Braheny S, Sipe J, Rice G, Huddlestone J, et al. Systemic alpha-interferon therapy of multiple sclerosis. Neurology. 1984;34(10):1273-.

13. de Veer MJ, Holko M, Frevel M, Walker E, Der S, Paranjape JM, et al. Functional classification of interferon-stimulated genes identified using microarrays. Journal of Leukocyte Biology. 2001;69(6):912-20.

14. Malmgaard L. Induction and regulation of IFNs during viral infections. Journal of Interferon & Cytokine Research. 2004;24(8):439-54.

15. Antonelli G. Biological basis for a proper clinical application of alpha interferons. New Microbiol. 2008;31(3):305-18.

16.Takaoka A, Yanai H. Interferon signalling network in innate defence. Cellular Microbiology. 2006;8(6):907-22.

17. Hardy MP, Owczarek CM, Jermiin LS, EjdebÃ¤ck M, Hertzog PJ. Characterization of the type I interferon locus and identification of novel genes. Genomics. 2004;84(2):331-45.

18. LaFleur DW, Nardelli B, Tsareva T, Mather D, Feng P, Semenuk M, et al. Interferon-κ, a novel type I interferon expressed in human keratinocytes. Journal of Biological Chemistry. 2001;276(43):39765-71.

19. Uze G, Schreiber G, Piehler J, Pellegrini S. The receptor of the type I interferon family. Current Topics in Microbiology and Immunology. 2007:71-95.

20. Samuel CE. Antiviral actions of interferons. Clinical Microbiology Reviews. 2001;14(4):778-809.

21. Silverman RH. Implications for RNase L in prostate cancer biology. Biochemistry. 2003;42(7):1805-12.

22. Williams BRG. Signal integration via PKR. Science's STKE. 2001;2001(89):re2.

23. Haller O, Staeheli P, Kochs G. Interferon-induced Mx proteins in antiviral host defense. Biochimie. 2007;89(6):812-8.

24. Sheppard P, Kindsvogel W, Xu W, Henderson K, Schlutsmeyer S, Whitmore TE, et al. IL-28, IL-29 and their class II cytokine receptor IL-28R. Nature Immunology. 2002;4(1):63-8.

25. Sun Q, Sun L, Liu HH, Chen X, Seth RB, Forman J, et al. The specific and essential role of MAVS in antiviral innate immune responses. Immunity. 2006;24(5):633-42.

26. Belardelli F, Gresser I. The neglected role of type I interferon in the T-cell response: implications for its clinical use. Immunology Today. 1996;17(8):369-72.

27. Fellous M, Nir U, Wallach D, Merlin G, Rubinstein M, Revel M. Interferon-dependent induction of mRNA for the major histocompatibility antigens in human fibroblasts and lymphoblastoid cells. Proceedings of the National Academy of Sciences. 1982;79(10):3082.

28. Zhao W, Cha EN, Lee C, Park CY, Schindler C. Stat2-dependent regulation of MHC class II expression. The Journal of Immunology. 2007;179(1):463-71.

29. Palmer KJ, Harries M, Gore ME, Collins MKL. Interferon-alpha (IFN-α) stimulates anti-melanoma cytotoxic T lymphocyte (CTL) generation in mixed lymphocyte tumour cultures (MLTC). Clinical & Experimental Immunology. 2000;119(3):412-8.

30. Romagnani S. Induction of TH1 and TH2 responses: a key role for the 'natural' immune response? Immunology Today. 1992;13(10):379-81.

31. Fleetwood AJ, Dinh H, Cook AD, Hertzog PJ, Hamilton JA. GM-CSF-and M-CSF-dependent macrophage phenotypes display differential dependence on type I interferon signaling. Journal of Leukocyte Biology. 2009;86(2):411-21.

32. Belardelli F, Vignaux F, Proietti E, Gresser I. Injection of mice with antibody to interferon renders peritoneal macrophages permissive for vesicular stomatitis virus and encephalomyocarditis virus. Proceedings of the National Academy of Sciences. 1984;81(2):602.

33. Li BL, Zhao XX, Liu XY, Kim HS, Raska K, Ortaldo JR, et al. Alpha-Interferon Structure and Natural Killer Cell Stimulatory Activity. Cancer Research. 1990;50(17):5328.

34. Belardelli F, Ferrantini M, Proietti E, Kirkwood JM. Interferon-alpha in tumor immunity and immunotherapy. Cytokine & growth factor reviews. 2002;13(2):119-34.

35. Rizza P, Moretti F, Belardelli F. Recent advances on the immunomodulatory effects of IFN-alpha: implications for cancer immunotherapy and autoimmunity. Autoimmunity.43(3):204-9.

36. McCarty MF, Bielenberg D, Donawho C, Bucana CD, Fidler IJ. Evidence for the causal role of endogenous interferon-alpha/beta in the regulation of angiogenesis,

tumorigenicity, and metastasis of cutaneous neoplasms. Clinical & Exprimental Metastasis. 2002;19(7):609-15.

37. Akira S, Uematsu S, Takeuchi O. Pathogen recognition and innate immunity. Cell. 2006;124(4):783-801.

38. Meylan E, Tschopp J, Karin M. Intracellular pattern recognition receptors in the host response. Nature. 2006;442(7098):39-44.

39. Matsumiya T, Stafforini DM. Function and regulation of retinoic acid-inducible gene-I. Critical Reviews in Immunology. 2010;30(6):489.

40. Rudd BD, Smit JJ, Flavell RA, Alexopoulou L, Schaller MA, Gruber A, et al. Deletion of TLR3 alters the pulmonary immune environment and mucus production during respiratory syncytial virus infection. The Journal of Immunology. 2006;176(3):1937-42.

41. Yoneyama M, Fujita T. Recognition of viral nucleic acids in innate immunity. Reviews in Medical Virology. 2010;20(1):4-22.

42. Kato H, Sato S, Yoneyama M, Yamamoto M, Uematsu S, Matsui K, et al. Cell type-specific involvement of RIG-I in antiviral response. Immunity. 2005;23(1):19-28.

43. Yoneyama M, Kikuchi M, Natsukawa T, Shinobu N, Imaizumi T, Miyagishi M, et al. The RNA helicase RIG-I has an essential function in double-stranded RNA-induced innate antiviral responses. Nature Immunology. 2004;5(7):730-7.

44. Honda K, Takaoka A, Taniguchi T. Type I Inteferon Gene Induction by the Interferon Regulatory Factor Family of Transcription Factors. Immunity. 2006;25(3):349-60.

45. Sato M, Suemori H, Hata N, Asagiri M, Ogasawara K, Nakao K, et al. Distinct and Essential Roles of Transcription Factors IRF-3 and IRF-7 in Response to Viruses for IFN-α/β Gene Induction. Immunity. 2000;13(4):539-48.

46. Garcin D, Lezzi M, Dobbs M, Elliott RM, Schmaljohn C, Kang CY, et al. The 5'ends of Hantaan virus (Bunyaviridae) RNAs suggest a prime-and-realign mechanism for the initiation of RNA synthesis. Journal of Virology. 1995;69(9):5754-62.

47. Hornung V, Ellegast J, Kim S, Brzózka K, Jung A, Kato H, et al. 5'-Triphosphate RNA is the ligand for RIG-I. Science's STKE. 2006;314(5801):994.

48. Pichlmair A, Schulz O, Tan CP, Naslund TI, Liljestrom P, Weber F, et al. RIG-I-mediated antiviral responses to single-stranded RNA bearing 5'-phosphates. Science's STKE. 2006;314(5801):997.

49. Kato H, Takeuchi O, Sato S, Yoneyama M, Yamamoto M, Matsui K, et al. Differential roles of MDA5 and RIG-I helicases in the recognition of RNA viruses. Nature. 2006;441(7089):101-5.

50. Takahasi K, Yoneyama M, Nishihori T, Hirai R, Kumeta H, Narita R, et al. Nonself RNA-sensing mechanism of RIG-I helicase and activation of antiviral immune responses. Molecular Cell. 2008;29(4):428-40.

51. Bork P, Koonin EV. An expanding family of helicases within the 'DEAD/H' superfamily. Nucleic Acids Research. 1993;21(3):751-2.

52. Jankowsky E, Jankowsky A. The DExH/D protein family database. Nucleic Acids Research. 2000;28(1):333-4.

53. Saito T, Hirai R, Loo YM, Owen D, Johnson CL, Sinha SC, et al. Regulation of innate antiviral defenses through a shared repressor domain in RIG-I and LGP2. Science's STKE. 2007;104(2):582.

54. Marques JT, Devosse T, Wang D, Zamanian-Daryoush M, Serbinowski P, Hartmann R, et al. A structural basis for discriminating between self and nonself double-stranded RNAs in mammalian cells. Nature Biotechnology. 2006;24(5):559-65.

55. Sumpter Jr R, Loo YM, Foy E, Li K, Yoneyama M, Fujita T, et al. Regulating intracellular antiviral defense and permissiveness to hepatitis C virus RNA replication through a cellular RNA helicase, RIG-I. Journal of Virology. 2005;79(5):2689-99.

56. Wang D, Boerner SA, Winkler JD, LoRusso PM. Clinical experience of MEK inhibitors in cancer therapy. Biochimica et Biophysica Acta (BBA)-Molecular Cell Research. 2007;1773(8):1248-55.

57. Cui S, Eisenächer K, Kirchhofer A, Brzózka K, Lammens A, Lammens K, et al. The C-terminal regulatory domain is the RNA 5'-triphosphate sensor of RIG-I. Molecular Cell. 2008;29(2):169-79.

58. Kawai T, Akira S. Innate immune recognition of viral infection. Nature Immunology. 2006;7(2):131-7.

59. Civril F, Bennett M, Moldt M, Deimling T, Witte G, Schiesser S, et al. The RIG-I ATPase domain structure reveals insights into ATP-dependent antiviral signalling. EMBO Reports. 2011.

60. Kumar H, Kawai T, Kato H, Sato S, Takahashi K, Coban C, et al. Essential role of IPS-1 in innate immune responses against RNA viruses. The Journal of Experimental Medicine. 2006;203(7):1795-803.